Meriem Durgud | Saurabh Gupta | Ivan Ivanov | M. Amin Omidbakhshfard | Maria Benina | Saleh Alseekh | Nikola Staykov Mareike Hauenstein | Paul P. Dijkwel | Stefan Hortensteiner Valentina Toneva | Yariv Brotman | Alisdair R. Fernie Bernd Müller-Röber | Tsanko S. Gechev

Molecular Mechanisms Preventing Senescence in Response to Prolonged Darkness in a Desiccation-Tolerant Plant

Suggested citation referring to the original publication:
Plant Physiology 177 (2018) 3, pp. 1319–1338
DOI https://doi.org/110.1104/pp.18.00055
ISSN (print) 0032-0889
ISSN (online) 1532-2548

Molecular Mechanisms Preventing Senescence in Response to Prolonged Darkness in a Desiccation-Tolerant Plant[1][OPEN]

Meriem Durgud,[a,b,c] Saurabh Gupta,[d] Ivan Ivanov,[a,b] M. Amin Omidbakhshfard,[d,e] Maria Benina,[a] Saleh Alseekh,[a,e] Nikola Staykov,[a,b] Mareike Hauenstein,[f] Paul P. Dijkwel,[g] Stefan Hörtensteiner,[f] Valentina Toneva,[a,b,c] Yariv Brotman,[h] Alisdair R. Fernie,[a,e] Bernd Mueller-Roeber,[a,d] and Tsanko S. Gechev[a,b,c,2]

[a]Center of Plant Systems Biology and Biotechnology, Plovdiv 4000, Bulgaria
[b]Institute of Molecular Biology and Biotechnology, Plovdiv 4000, Bulgaria
[c]Department of Plant Physiology and Molecular Biology, University of Plovdiv, Plovdiv 4000, Bulgaria
[d]Department Molecular Biology, Institute of Biochemistry and Biology, University of Potsdam, 14476 Potsdam, Germany
[e]Department Willmitzer, Max Planck Institute of Molecular Plant Physiology, 14476 Potsdam, Germany
[f]Department of Plant and Microbial Biology, University of Zurich, CH-8008 Zurich, Switzerland
[g]Institute of Fundamental Sciences, Massey University, 4474 Palmerston North, New Zealand
[h]Department of Life Sciences, Ben Gurion University of the Negev, Beersheva, Israel

ORCID IDs: 0000-0001-5214-2738 (I.I.); 0000-0003-2067-5235 (S.A.); 0000-0003-1617-2993 (N.S.); 0000-0002-0044-0490 (M.H.); 0000-0002-1432-2209 (P.P.D.); 0000-0001-9000-335X (A.R.F.) (A.R.F.); 0000-0002-1410-464X (B.M.) (B.M.); 0000-0002-3328-0243 (T.S.G.)

The desiccation-tolerant plant *Haberlea rhodopensis* can withstand months of darkness without any visible senescence. Here, we investigated the molecular mechanisms of this adaptation to prolonged (30 d) darkness and subsequent return to light. *H. rhodopensis* plants remained green and viable throughout the dark treatment. Transcriptomic analysis revealed that darkness regulated several transcription factor (TF) genes. Stress- and autophagy-related TFs such as *ERF8*, *HSFA2b*, *RD26*, *TGA1*, and *WRKY33* were up-regulated, while chloroplast- and flowering-related TFs such as *ATH1*, *COL2*, *COL4*, *RL1*, and *PTAC7* were repressed. *PHYTOCHROME INTERACTING FACTOR4*, a negative regulator of photomorphogenesis and promoter of senescence, also was down-regulated. In response to darkness, most of the photosynthesis- and photorespiratory-related genes were strongly down-regulated, while genes related to autophagy were up-regulated. This occurred concomitant with the induction of SUCROSE NON-FERMENTING1-RELATED PROTEIN KINASES (SnRK1) signaling pathway genes, which regulate responses to stress-induced starvation and autophagy. Most of the genes associated with chlorophyll catabolism, which are induced by darkness in dark-senescing species, were either unregulated (*PHEOPHORBIDE A OXYGENASE, PAO; RED CHLOROPHYLL CATABOLITE REDUCTASE, RCCR*) or repressed (*STAY GREEN-LIKE*, *PHEOPHYTINASE*, and *NON-YELLOW COLORING1*). Metabolite profiling revealed increases in the levels of many amino acids in darkness, suggesting increased protein degradation. In darkness, levels of the chloroplastic lipids digalactosyldiacylglycerol, monogalactosyldiacylglycerol, phosphatidylglycerol, and sulfoquinovosyldiacylglycerol decreased, while those of storage triacylglycerols increased, suggesting degradation of chloroplast membrane lipids and their conversion to triacylglycerols for use as energy and carbon sources. Collectively, these data show a coordinated response to darkness, including repression of photosynthetic, photorespiratory, flowering, and chlorophyll catabolic genes, induction of autophagy and SnRK1 pathways, and metabolic reconfigurations that enable survival under prolonged darkness.

Abiotic stresses, such as dehydration, starvation, and darkness, induce premature senescence in most angiosperms. In Arabidopsis (*Arabidopsis thaliana*), darkness triggers chlorophyll degradation, senescence, and cell death within days of the switch from light to dark. The process is regulated by a number of proteins, including transcription factors (TFs) and microRNAs (Ishizaki et al., 2005; Sakuraba et al., 2014; Song et al., 2014; Huo et al., 2015). Rapid chlorophyll loss and senescence symptoms days after the imposition of dark treatment also are observed in other model and crop species, including common bean (*Phaseolus vulgaris*) and rice (*Oryza sativa*; Denev et al., 2012; Talla et al., 2016).

Long-term darkness inevitably leads to carbon and energy starvation when starch reserves are exhausted. Hence, plants must use alternative nutrient and energy sources to survive long periods of darkness. In Arabidopsis plants subjected to extended darkness, amino acids and fatty acids are used as alternative respiratory substrates (Kunz et al., 2009; Araújo et al., 2010; Fan et al., 2017). Mutants perturbed in the degradation of branched-chain amino acids, Lys, and phytol are more sensitive to extended darkness and exhibit early senescence, as evidenced by enhanced bleaching, chlorophyll loss, and cell death (Araújo et al., 2010, 2011). Likewise, fatty acid β-oxidation is essential for plant survival in darkness, as the *peroxisomal ABC-transporter1* and *keto-acyl-thiolase2* mutants, defective in peroxisomal β-oxidation, develop necrosis and die after an extended period of darkness that was not lethal for wild-type plants (Kunz et al., 2009). Autophagy is an important mechanism that breaks down proteins and lipids and, thereby, provides the cell with alternative carbon, nitrogen, and energy during extended

darkness (Avin-Wittenberg et al., 2015; Barros et al., 2017; Schwarz et al., 2017).

Angiosperm resurrection species can tolerate massive desiccation down to a relative water content (RWC) as low as 5% and recover fully upon rewatering (Gechev et al., 2012). *Haberlea rhodopensis* is a perennial dicotyledonous species from the family Gesneriaceae and is closely related to the recently sequenced species *Dorcoceras hygrometricum* (*Boea hygrometrica*; Xiao et al., 2015). *H. rhodopensis* is endemic to mountains in the Balkan peninsula (southeastern Europe), where it lives mainly in the undergrowth (Georgieva et al., 2017). *H. rhodopensis* also can tolerate freezing temperatures during the winter and high levels of oxidative stress (Benina et al., 2013; Gechev et al., 2013). In contrast to other species, the integrity and activity of the photosynthetic apparatus of the desiccation-tolerant *H. rhodopensis* is preserved months after darkness, and no visible senescence symptoms are observed during this time period (Denev et al., 2012). Such tolerance to long-term darkness is rarely seen in angiosperms, and the molecular mechanisms behind this phenomenon have not been studied.

Here, we investigated the transcriptomic and metabolomic reprogramming of *H. rhodopensis* during short- and long-term darkness and subsequent recovery in order to identify genes and metabolic pathways potentially involved in the adaptive response to prolonged darkness. We focus our discussion on processes such as photosynthesis and photorespiration, growth and energy regulation, carbohydrate and lipid metabolism, protein degradation, and autophagy in an attempt to postulate a model for how *H. rhodopensis* rewires its primary energy metabolism to withstand extreme periods of darkness.

RESULTS

H. rhodopensis Tolerates Long-Term Darkness

Intact *H. rhodopensis* plants, grown under optimal conditions (16-h-light/8-h-dark periods, 30–35 µmol m^{-2} s^{-1} light intensity, and 22°C), were subjected to complete darkness for 30 d (dark stress) and then transferred back to optimal conditions under light for 7 d (recovery). In parallel, another set of plants was grown at optimal conditions throughout the whole experiment to provide the proper developmental time controls. Plant samples were taken just before the start of the dark-stress treatment (T0 controls), following 7 d of treatment (short-term darkness) or 30 d of treatment (long-term darkness), and 7 d after the return to light after the long-term dark treatment (recovery). The same sampling timing was used for the control plants not subjected to darkness. Intriguingly, both plants grown at optimal conditions throughout the whole period and plants exposed to darkness for 1 month and a subsequent 1-week recovery remained green and viable (Fig. 1). The control plants grown at optimal conditions continued to grow well, as indicated by the increased rosette leaf size. These plants gained fresh weight (Table I) and their leaves appeared bigger and wider (Fig. 1).

The plants cultivated in darkness had narrower and slightly more elongated leaves than did plants grown in photoperiod (Fig. 1). Interestingly, the plants grown in darkness also gained fresh weight, although less than that gained by the control plants (Table I). After 30 d in darkness, the plants remained green, although they appeared slightly paler than the controls (Fig. 1B). Their leaves were a bit more elongated and slightly curled, while the leaves of control plants grown under photoperiod were not elongated. However, the tissue firmness of the plants grown in darkness was similar to that of the control leaves. Measurements of the chlorophyll content showed only a 30% reduction in total chlorophyll levels in the dark-grown plants as compared with the untreated control plants (Fig. 2A). As the chlorophyll *a*-to-chlorophyll *b* ratio may vary depending on the light regime, we determined the amount of chlorophyll *a* and chlorophyll *b* at the different time points and light/dark regimes. The chlorophyll *a*-to-chlorophyll *b* ratio was about 1.4 for all time points and conditions, including the controls and plants grown in darkness, which is similar to the chlorophyll *a*-to-chlorophyll *b* ratio observed by Denev et al. (2012). No accumulation of anthocyanins was detected in darkness (data not shown). Chlorophyll fluorescence values were 0.84 for the control plants, after 7 d of darkness, and after recovery, indicating a healthy PSII. After 30 d of darkness, the chlorophyll fluorescence value was 0.7, indicating stress. Measurements of electrolyte leakage failed to detect any increased conductivity in the dark-treated plants compared with the control, which shows that the prolonged darkness did not result in membrane damage (Fig. 2B). In a

[1]M.D., P.P.D., B.M.-R., and T.S.G. acknowledge the European Union's FP7 Project PlantAgeing (grant no. 612630). We thank the European Union's Horizon 2020 research and innovation program, Project PlantaSYST (SGA-CSA No. 739582 under FPA No. 664620). S.G. received funding from the European Union's Horizon 2020 Project CropStrengthen (grant no. 642901). S.H., B.M.-R., and T.S.G. also acknowledge Project AbioSen (ERA-CAPS).

[2]Address correspondence to tsangech@uni-plovdiv.bg.

The author responsible for distribution of materials integral to the findings presented in this article in accordance with the policy described in the Instructions for Authors (www.plantphysiol.org) is: Tsanko Gechev (tsangech@uni-plovdiv.bg).

M.D., I.I., A.O., and N.S. prepared the cultures and performed the stress treatment, the physiological experiments, and isolated RNA for the transcriptome analysis; S.G. analyzed the RNA-seq data sets; M.B., S.A., and A.R.F. prepared the metabolome samples and conducted the GC-MS analysis; M.H. and S.H. performed the phyllobilin analysis; A.O. and Y.B. performed the lipid profiling; T.S.G. designed the experiments, provided most of the funding, and analyzed the data; P.P.D., B.M.-R., and A.R.F. provided resources and contributed to the data interpretation; all authors wrote the article.

[OPEN]Articles can be viewed without a subscription.

www.plantphysiol.org/cgi/doi/10.1104/pp.18.00055

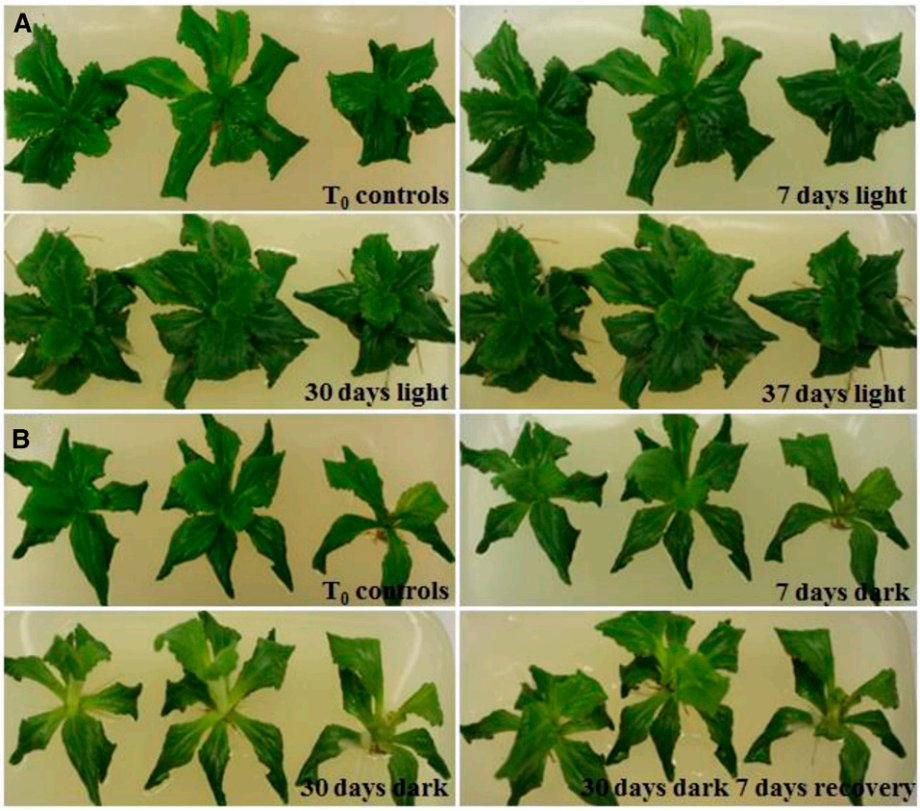

Figure 1. *H. rhodopensis* can survive long-term darkness without visible damage. A, Plants grown under the photoperiodic condition (16 h of light/8 h of dark) for up to 37 d. B, Plants kept in darkness for up to 1 month and then transferred to light (16-h-light/8-h-dark photoperiod) for 7 d (recovery).

parallel experiment, *H. rhodopensis* plants were exposed to desiccation under photoperiod and to desiccation in darkness. The conductivity of well-hydrated dark-treated plants was even less than the conductivity observed in the desiccated plants (Fig. 3). In another experiment, Arabidopsis plants were grown in darkness, which led to a rapid loss of chlorophyll after 3 d, with complete pigment loss after 3 weeks of darkness (Supplemental Fig. S1). All Arabidopsis plants failed to recover after subsequent transfer to the light and died shortly thereafter.

The 30% reduction in chlorophyll suggested that the chlorophyll may be partially degraded. In Arabidopsis and other dark-sensitive species, chlorophyll is degraded massively and chlorophyll degradation products (phyllobilins) can be detected (Hörtensteiner, 2013). Using a recently established liquid chromatography-mass spectroscopy procedure for the detection of phyllobilins in Arabidopsis (Christ et al., 2016), we identified a single nonfluorescent chlorophyll catabolite, NCC_806 (Supplemental Fig. S2), in our *H. rhodopensis* plants, which also accumulates as a minor catabolite in Arabidopsis. However, NCC_806 was already present in the T0 samples and decreased transiently following 7 d of darkness, with higher levels observed in samples harvested following recovery from the long-term dark stress.

Taken together, these results collectively show that, in sharp contrast with other plants, long-term darkness does not induce typical chlorophyll degradation and senescence in *H. rhodopensis*.

Table I. Fresh weight of *H. rhodopensis* plants grown in the photoperiod or in darkness

T0 are the unstressed controls at the beginning of the experiment. Asterisks indicate statistically significant differences from the T0 controls (**, $P < 0.01$) according to ANOVA with Tukey's honestly significant difference posthoc test. Values are means ± SD of 10 individual plants each.

Parameter	Treatment/ Time Point						
	T0 Controls	7 d of Light	30 d of Light	37 d of Light	7 d of Dark	30 d of Dark	30 d of Dark + 7 d of Light
Fresh weight (mg)	470 ± 80	580 ± 140	790 ± 110**	790 ± 160**	530 ± 200	610 ± 130**	630 ± 130**

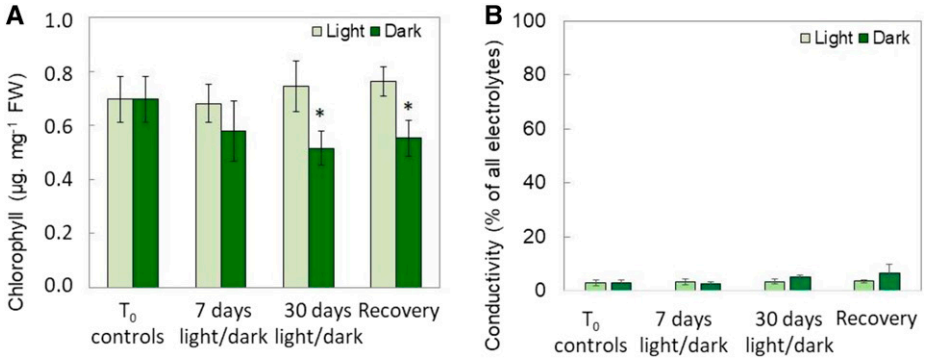

Figure 2. Darkness does not cause cell damage and significant chlorophyll loss in *H. rhodopensis*. A, Chlorophyll content in *H. rhodopensis* leaves during dark treatment and subsequent recovery. Data are means of 15 individual plants from three biological replicates. Error bars indicate SD. Asterisks indicate statistically significant differences from the respective light controls ($P < 0.05$, Student's *t* test). FW, Fresh weight. B, Conductivity of *H. rhodopensis* leaves during dark treatment and subsequent recovery. Data are means of three biological replicates. Error bars indicate SD.

H. rhodopensis Preserves Its Tolerance to Desiccation during Darkness

As *H. rhodopensis* is a desiccation-tolerant species, we examined if the desiccation tolerance is maintained during long-term exposure to darkness. To this end, plants exposed to 7 and 30 d of darkness, as well as plants subjected to 30 d of darkness followed by recovery, were left to desiccate to the air-dried state (Fig. 3). All light- and dark-grown plants that were not subjected to desiccation had an RWC between 83% and 86%, as is typically observed for well-hydrated *H. rhodopensis* (Gechev et al., 2013). Plants exposed to desiccation, regardless of the light conditions, had an RWC of about 5% (Fig. 3B). Conductivity measurements showed very little ion leakage in plants desiccated in the light and even lower values in plants desiccated in darkness (Fig. 3C). Both plants desiccated in the light or darkness recovered successfully upon rehydration and fully restored their RWC, demonstrating that the resurrection potential of *H. rhodopensis* is fully preserved in darkness.

RNA Sequencing and Assembly of the *H. rhodopensis* Transcriptome

To determine the transcriptional reprogramming as a result of the dark stress and subsequent recovery, we performed transcriptome analysis by RNA sequencing (RNA-seq) using Illumina technology. As the *H. rhodopensis* genome has not been sequenced, we performed a de novo transcriptome assembly of the obtained short-sequence reads. First, all reads were assessed for quality using FastQC (https://www.bioinformatics.babraham.ac.uk/projects/fastqc/) and an in-house script. The reads exhibited very high quality, and no further filtering was required (Supplemental Table S1). The reads from all samples were pooled and assembled into a single transcriptome using Trinity software with different *k*-mers (25, 27, 29, and 31). Potential redundancies were removed using the CD-HIT-EST program (Fu et al., 2012). Assemblies were evaluated to select the best assembly, using basic assembly statistics, and read alignment and completeness of assembly were evaluated by BUSCO using the embryophyta_odb9 data set (downloaded from http://busco.ezlab.org; Supplemental Table S1). All *k*-mers produced good quality assemblies, but *k*-mer 31 had better statistics than the others and, therefore, was selected for further analysis (Supplemental Table S1; Supplemental Fig. S3). The assembly produced 88,228 putative transcripts, accounting for 52,478 genes (similar to the number of genes reported for *D. hygrometricum*, a relative of *H. rhodopensis*, also from the family Gesneriaceae; Supplemental Table S1), after filtering out potential assembly artifacts (see "Materials and Methods"), with an average contig length of 1,452 bp and an N50 (minimum contig length to cover 50% of the transcriptome) of 2,022 bp. BUSCO analysis shows that 83.6% of highly conserved plant orthologs were complete, 6.2% were fragmented, and 10.2% were missing (Supplemental Table S1). All reads were pseudoaligned to the assembly using the kallisto program (Bray et al., 2016), with an average alignment percentage of 87% (Supplemental Fig. S3). These statistics indicate that the assembly is of sufficient quality to perform differential expression analysis.

About 84% of the transcripts had a BLAST hit against the National Center for Biotechnology Information nonredundant (NCBI nr) database; all of them also were found in the UniProt (Swissprot + TrEMBL) database. As expected, most transcripts (51%) were similar to the recently published *D. hygrometricum* genome, about 16% of the genes were most similar to *Sesamum indicum*, and 4% showed the highest similarity to *Erythranthe guttata* (Fig. 4). A substantial percentage of the transcripts (16.14%) had no similarity to any other species, suggesting that they may be specific to *H. rhodopensis*. Such genes occurring only in one or in a few taxonomically related species are known as

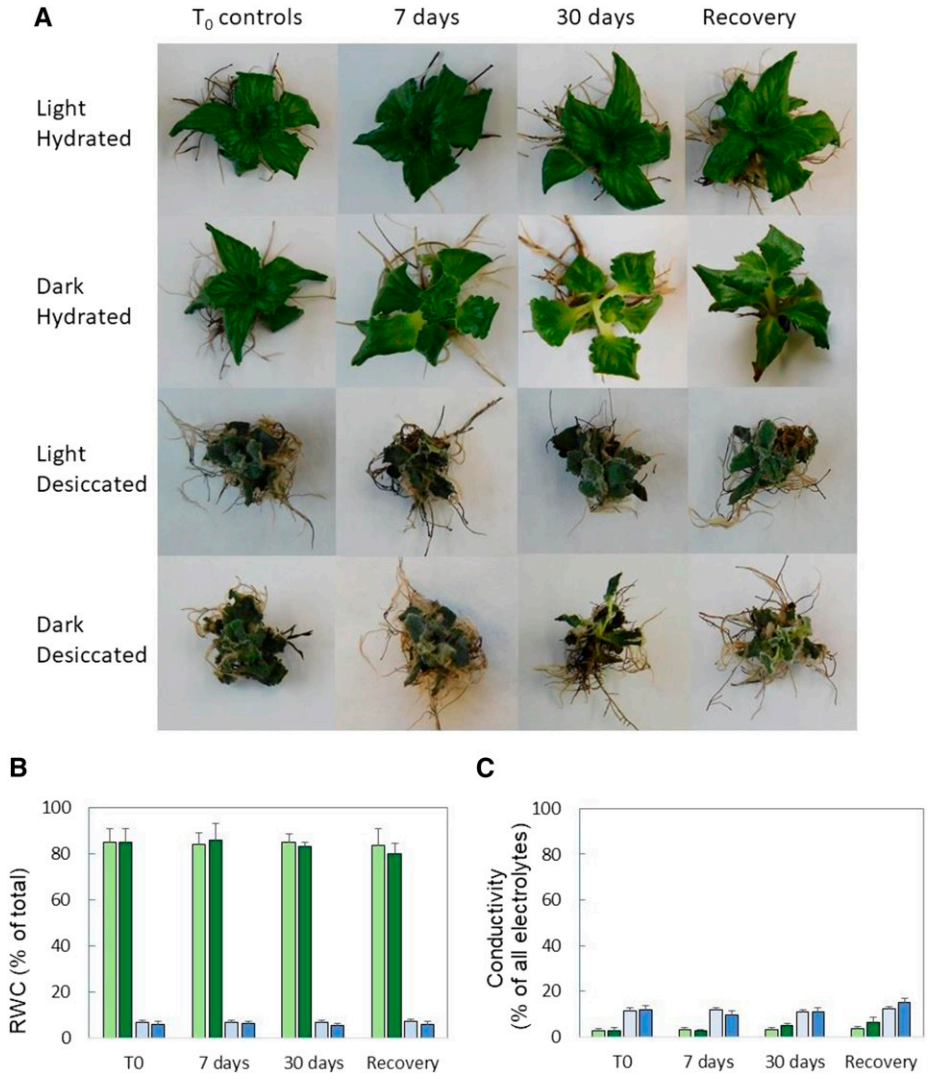

Figure 3. *H. rhodopensis* can tolerate desiccation in darkness. A, Phenotypes of hydrated and desiccated *H. rhodopensis* plants grown in the photoperiod (light) or in darkness. B, RWC of hydrated and desiccated *H. rhodopensis* plants grown in the photoperiod or in darkness. C, Electrolyte leakage (conductivity) of hydrated and desiccated *H. rhodopensis* plants grown in the photoperiod or in darkness. Data are means of three biological replicates. Error bars indicate SD.

taxonomically restricted genes (TRGs). The TRGs also are abundant in the resurrection species *Craterostigma plantagineum*, and some of them have been suggested to contribute to desiccation tolerance (Giarola et al., 2015).

Transcriptome Reconfigurations during Long-Term Darkness and Subsequent Recovery

The sample correlation matrix of the biological replicates showed similar gene expression at the two darkness time points, while the control (unstressed) samples were similar to the samples experiencing recovery from the darkness treatment (Supplemental Fig. S4). The transcripts from the plants subjected to dark stress and subsequent recovery were normalized against their respective time controls grown under optimal conditions and clustered according to their gene-level expression (Supplemental Fig. S5). We identified 9,334 differentially expressed genes (DEGs) across different pairwise combinations, similar to the number of DEGs reported in *D. hygrometricum* under desiccation stress. A large number of genes were differentially expressed after 7 and 30 d of darkness (7 d, 3,181 and 3,858 genes up- and down-regulated at least 2-fold, respectively; 30 d, 2,094 and 4,769 genes up- and down-regulated 2-fold, respectively; Fig. 5; Supplemental Table S2). Very few genes were differentially expressed at the recovery stage compared with their time control (80 and 289 genes up- and down-regulated 2-fold, respectively). The DEGs from all time points were clustered (Fig. 5), and Gene Ontology (GO)

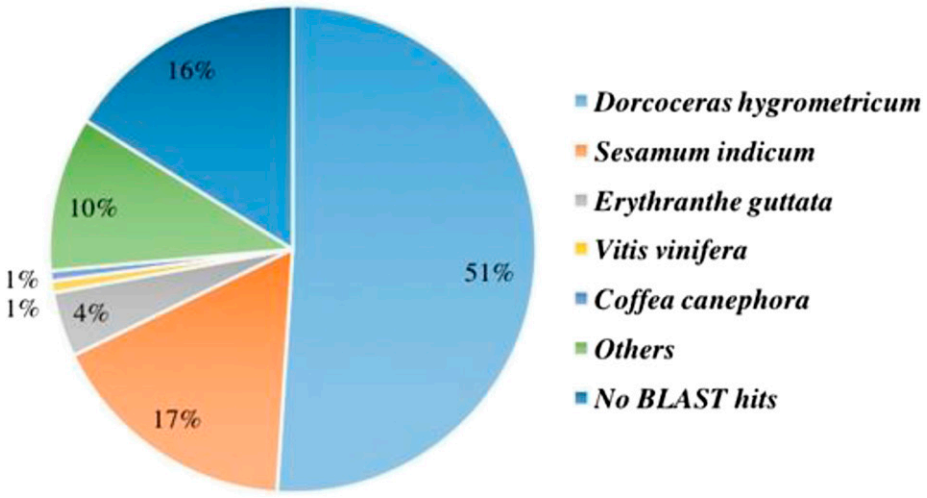

Figure 4. Species distribution of top BLASTX hits of *H. rhodopensis* transcripts against the NCBI nr database. *H. rhodopensis* transcripts were computationally translated into all possible protein sequences and compared with protein sequences in the NCBI nr database using BLASTX. The pie chart shows the percentages of the best BLAST hits from different species.

enrichment was performed using GOSeq in order to gain insight into the cellular processes involved.

GO enrichment revealed a large number of enriched GO terms among the down-regulated genes during darkness. Some of the highly enriched GO terms include photosynthesis, chlorophyll biosynthetic process, photorespiration, ribulose-bisphosphate carboxylase activity, and endopeptidase inhibitor activity. Very few GO terms were enriched in up-regulated genes during darkness, which include DNA binding TF activity, protein-tetrapyrrole linkage, gibberellic acid mediated signaling pathway, and calcium-transporting ATPase

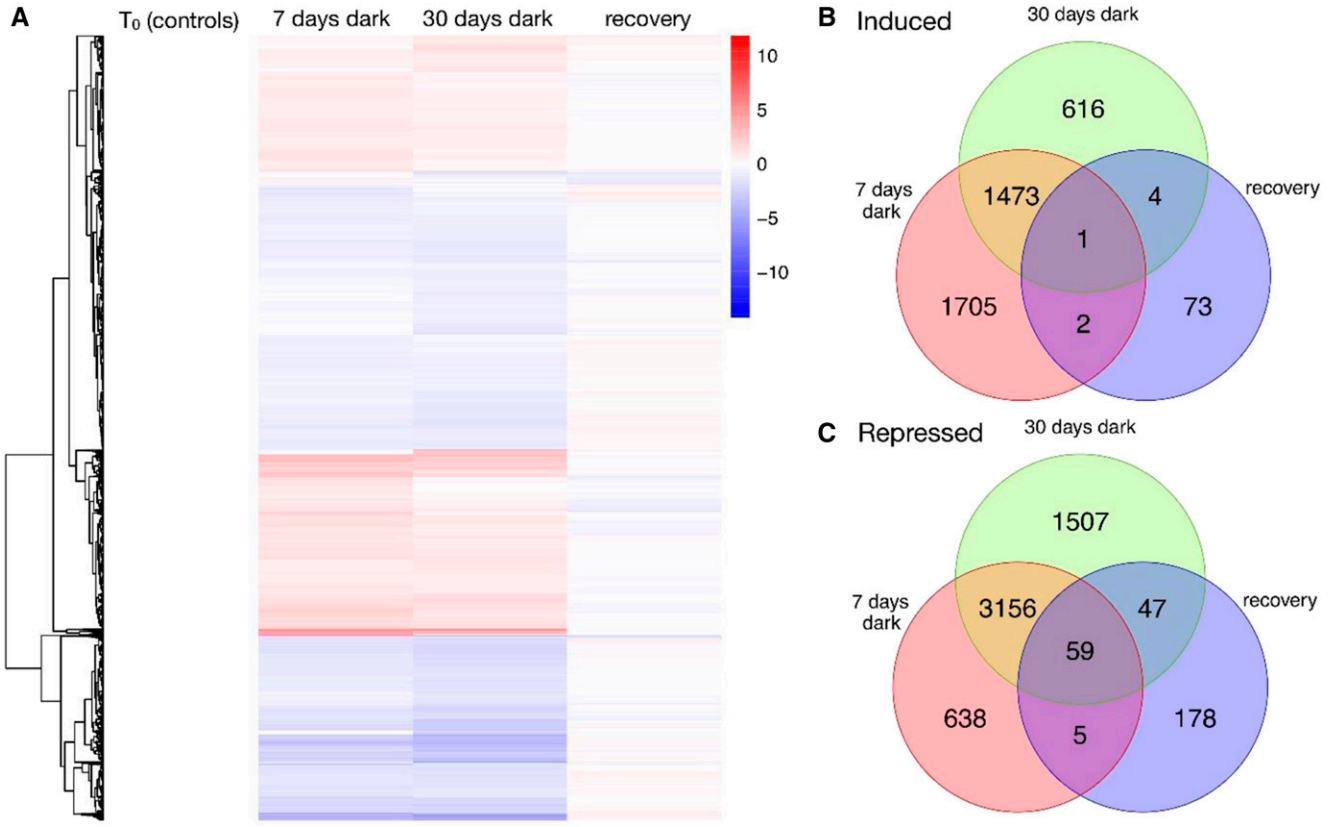

Figure 5. DEGs in at least one of the three conditions (7 d of darkness, 30 d of darkness, and recovery from darkness). A, Values plotted are $\log_2$ fold change, where T0 values = 0. Values are statistically significant ($P < 0.05$, Student's *t* test). B, Venn diagram of up-regulated DEGs, C, Venn diagram of down-regulated DEGs.

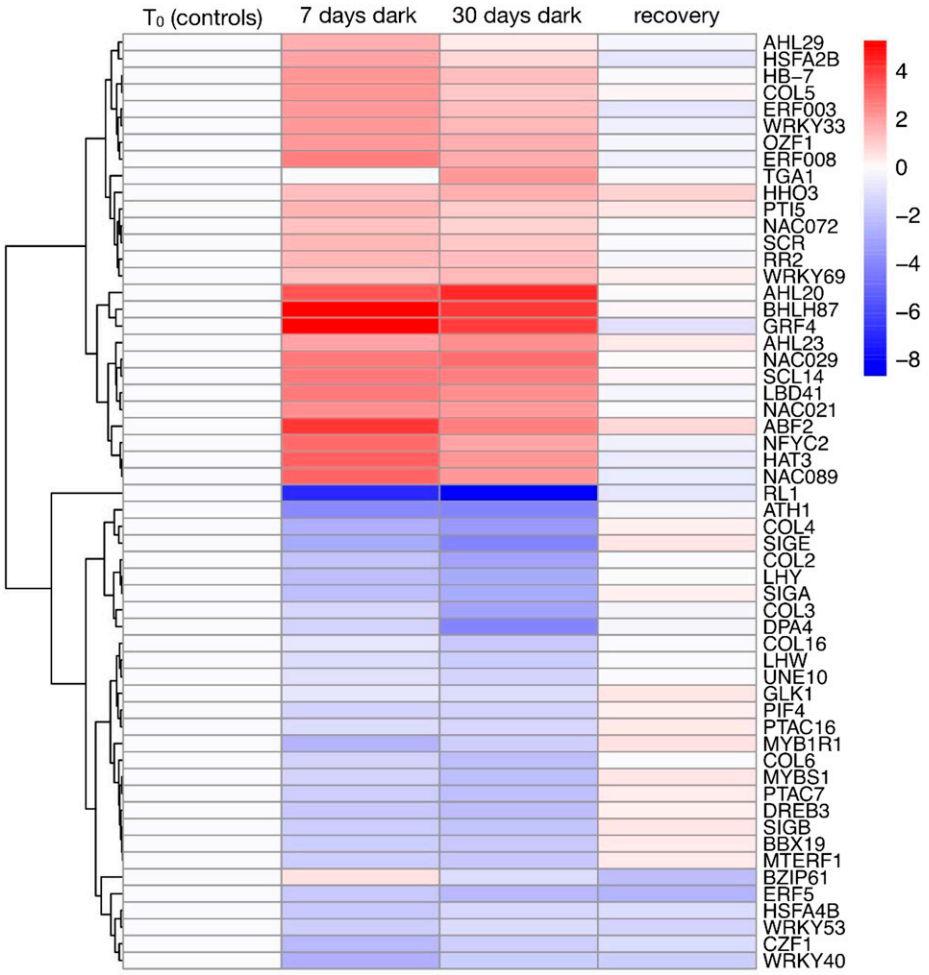

Figure 6. Differentially expressed TF genes in at least one of the three conditions (7 d of darkness, 30 d of darkness, and recovery from darkness). Values plotted are $\log_2$ fold change, where T0 values = 0.

activity (Supplemental Table S3). Interestingly, 1,271 of the highly regulated genes in darkness were specific to *H. rhodopensis*, with no sequence similarities to other species.

The assembled transcriptome includes 2,771 genes potentially encoding for TFs, 601 of which were differentially expressed in at least one pairwise combination. Some of the strongly dark-induced or -repressed TF-encoding genes are listed in Figure 6 (Supplemental Table S4), which may have roles in the massive transcriptional reprogramming that renders *H. rhodopensis* tolerant to long-term darkness.

The two most highly up-regulated genes among the TFs (47-fold induction after 7 d of darkness for both genes) had sequence similarity to the Arabidopsis *GROWTH REGULATING FACTOR4* and a basic helix-loop-helix (bHLH) family protein of unknown function (*BHLH87*). Two other genes highly induced by darkness had similarities to the Arabidopsis TF genes *ANAC029* and *WRKY33*. Also, several ethylene- and stress-related TF genes (*ETHYLENE RESPONSE FACTOR3* [*ERF3*], *ERF8*, *HEAT SHOCK FACTOR A2b*, *PATHOGENESIS-RELATED GENES TRANSCRIPTIONAL ACTIVATOR5*, *RESPONSIVE TO DESICCATION26* [*RD26*], and *TGACG-BINDING FACTOR1* [*TGA1*]) were induced (Fig. 6; Supplemental Tables S1 and S4).

Cell cycle-related genes were generally unaltered in darkness (Supplemental Table S1), which was in accordance with the observation that plants gain fresh weight and still grow in this condition. However, a few growth- and cell expansion-related genes, such as a gene with homology to Arabidopsis *XYLOGLUCAN ENDOTRANSGLUCOSYLASE/HYDROLASE9*, were even induced in darkness (Supplemental Table S2).

Many of the down-regulated genes were related to light signaling and chloroplasts: PROTEIN PLASTID TRANSCRIPTIONALLY ACTIVE7 (PTAC7), PTAC16, PHYTOCHROME INTERACTING FACTOR4 (PIF4), and chloroplastic TRANSCRIPTION TERMINATION FACTOR MTERF1 (Fig. 6; Supplemental Tables S1 and

S3). The key photomorphogenesis TF gene GOLDEN2-LIKE1 (GLK1; Martín et al., 2016) also was moderately repressed by darkness (Fig. 6; Supplemental Table S1). Furthermore, a number of genes with sequence similarities to Arabidopsis flowering-related TFs were down-regulated: ARABIDOPSIS ABC2 HOMOLOG1, CONSTANS-LIKE2 (COL2), COL4, and RADIALIS (RL1; Fig. 6).

Pathway analysis revealed the up-regulation of genes related to processes such as autophagy and protein degradation, while genes related to processes such as photosynthesis and photorespiration were heavily down-regulated (Fig. 7). In particular, several genes encoding autophagy (ATG) proteins were induced (*ATG13b* and *ATG18d*), as well as *WRKY33*, which encodes an autophagy-related TF in Arabidopsis (Lai et al., 2011). Photosynthesis-related genes were strongly down-regulated, as evidenced by the repression of genes encoding subunits of PSI and PSII reaction centers, the small Rubisco subunit, light-harvesting complex proteins, chlorophyll *a*/*b*-binding proteins, carbonic anhydrases, and many others (Fig. 7). Concomitantly, many key genes from the photorespiratory pathway were repressed, including genes encoding chloroplastic phosphoglycolate phosphatase, peroxisomal catalase, and chloroplastic glycerate kinase (Fig. 7).

A number of genes encoding photoreceptors (*PHYTOCHROME A*, *PHYTOCHROME B*, and *CRYPTOCHROME2*) were induced. At the same time, *PIF4*, which encodes the repressor of photomorphogenesis, was down-regulated.

A lack of photosynthesis would ultimately deplete starch, which, as for most plant species, is the main storage carbohydrate of *H. rhodopensis*. Genes involved in starch synthesis, such as those encoding phosphoglucomutases, ADP-Glc pyrophosphorylases, and starch synthases, as well as genes involved in starch degradation (e.g. α- and β-amylases) were repressed in darkness (Fig. 7). Regarding Suc and trehalose metabolism, several Suc synthase-encoding genes were strongly induced while genes encoding trehalose 6-phosphate synthase and trehalose 6-phosphate phosphatase were induced (Fig. 7).

Plant lipids are functionally diverse, fulfilling various roles from carbon and energy storage to structural and signaling functions. Only a few genes encoding enzymes related to lipid metabolism were induced, including genes encoding a lipase and a phospholipase (Fig. 7). More lipid-related genes were actually down-regulated during the dark treatment compared with controls, including genes encoding desaturases, phospholipase A and phospholipase D isoforms, a gene encoding a plastid-lipid associated protein, a gene encoding a galactolipid galactosyltransferase, and an esterase/lipase gene (Fig. 7). The expression of most of the other lipid-related genes did not vary.

Given that long-term darkness induces senescence in many plant species, we next focused on genes related to chlorophyll degradation and senescence. There was no indication of premature aging/senescence, since most of the genes either exhibited invariant expression or were repressed. The expression of the key chlorophyll-degrading genes *PAO* and *RCCR* was unaltered, while other chlorophyll catabolism genes, such as *SGRL*, *PPH*, and *NYC1*, were repressed (Table I).

As many abiotic stresses, including darkness, and senescence are linked with transient or sustained oxidative stress, we looked at the expression patterns of key antioxidant genes such as *SUPEROXIDE DISMUTASE* (*SOD*), *CATALASE* (*CAT*), *DEHYDROASCORBATE REDUCTASE* (*DHAR*), *GLUTATHIONE PEROXIDASE* (*GPX*), *GLUTATHIONE-S-TRANSFERASE* (*GST*), and *GLUTATHIONE REDUCTASE*. Antioxidant genes often are induced by various stresses, but in *H. rhodopensis*, most of these genes were either unaltered or repressed (Fig. 6). Only a small number of the genes encoding for mitochondrial *MnSOD* and a few *GPX* genes were induced (Fig. 7). The chloroplastic *Cu/ZnSOD* and *FeSOD*, the peroxisomal *CAT*, a *DHAR* gene, and a few *GPX* and *GST* genes were repressed (Fig. 7).

Metabolome Reconfiguration during Long-Term Darkness and Subsequent Recovery

We observed dramatic changes in a number of metabolites following the dark treatment. Sample clustering revealed that the two darkness time points are very close together yet distinct from the recovery samples, which more closely resembled the control light-grown samples (Supplemental Fig. S6), which was in accordance with observations from the transcriptome data (Supplemental Fig. S4).

Most notably, many amino acids increased in abundance during the period of extended darkness, and the high levels of some of them were sustained in the subsequent recovery. Fourteen of the proteinogenic amino acids were at a higher level in one or both of the darkness time points, and four of them (Arg, Asn, Lys, and Met) also displayed higher levels following the recovery period (Fig. 8) (Supplemental Table S5). Only two amino acids, namely Ala and Ser, decreased in abundance following the imposition of long-term darkness.

While Suc levels remained unaltered throughout the experiment, a few sugars, such as Glc, Xyl, and raffinose, increased as a result of the dark treatment. The high Glc levels were retained at the recovery time point. Trehalose levels were lower both after 1 week of darkness and after recovery (Fig. 8). Two polyvalent alcohols, namely mannitol and myo-inositol, increased in abundance in darkness. Dehydroascorbate levels also were higher in darkness, and this was maintained during recovery (Fig. 8). By contrast, γ-aminobutyric acid and two organic acids of the tricarboxylic acid cycle, malic acid and succinic acid, decreased in darkness (Fig. 8). A reconstructed metabolic map illustrating these data is presented in Figure 9.

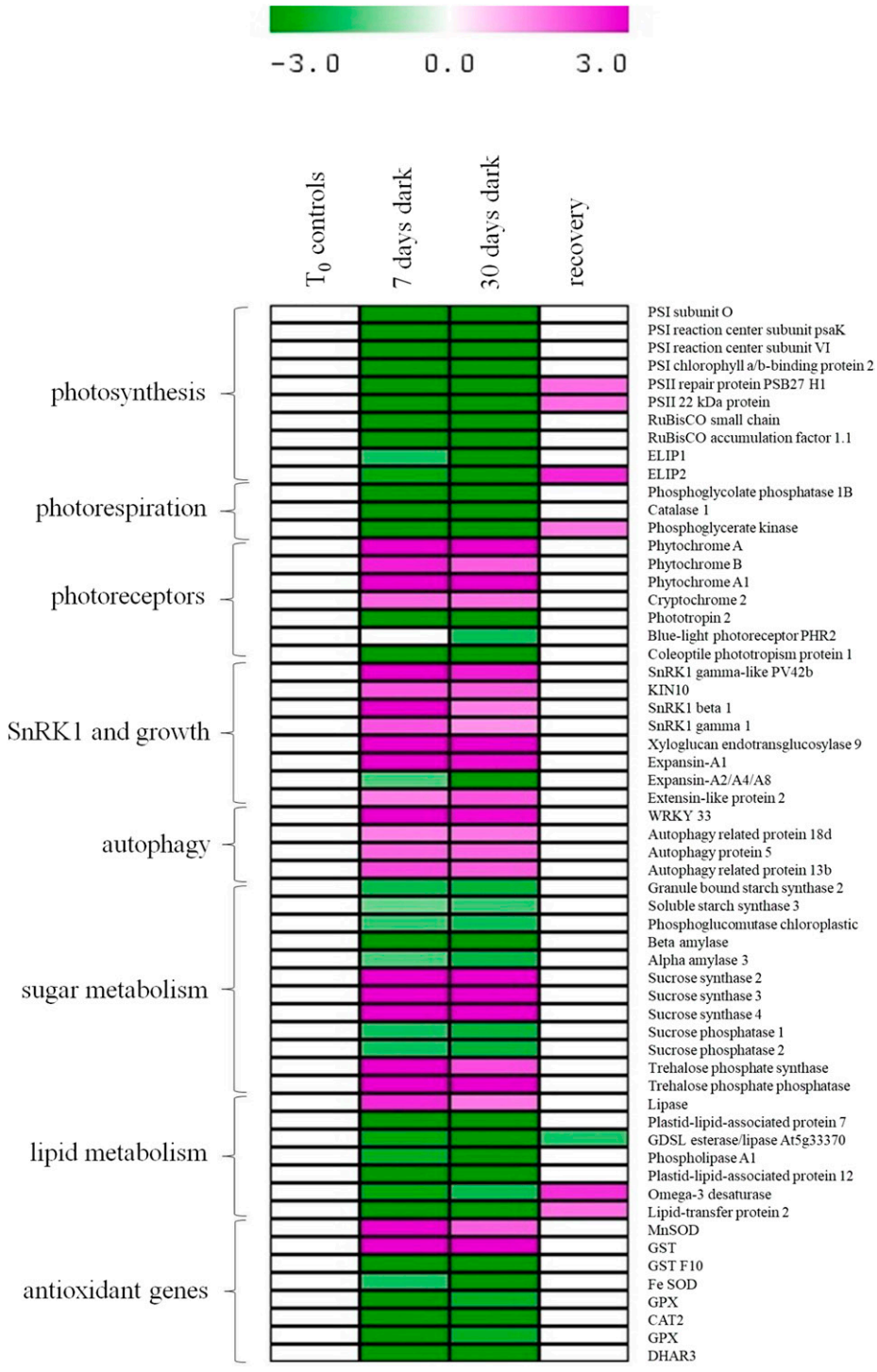

Figure 7. Expression of key genes representing pathways significantly regulated during long-term darkness and subsequent recovery in *H. rhodopensis*. Magenta and green depict gene induction and repression, respectively, compared with the control plants grown under the photoperiod and measured at the same time points. The data are means of three biological replicates.

Alterations of Lipids during Darkness and Subsequent Recovery

As lipids are important for energy metabolism and also represent key structural and signaling molecules, we determined the lipidome alterations during darkness and subsequent recovery. In total, 143 annotated lipids from the 10 neutral and polar lipid classes were identified. Neutral lipids of the diacylglycerol and triacylglyceride (TAG) classes, as well as polar lipids

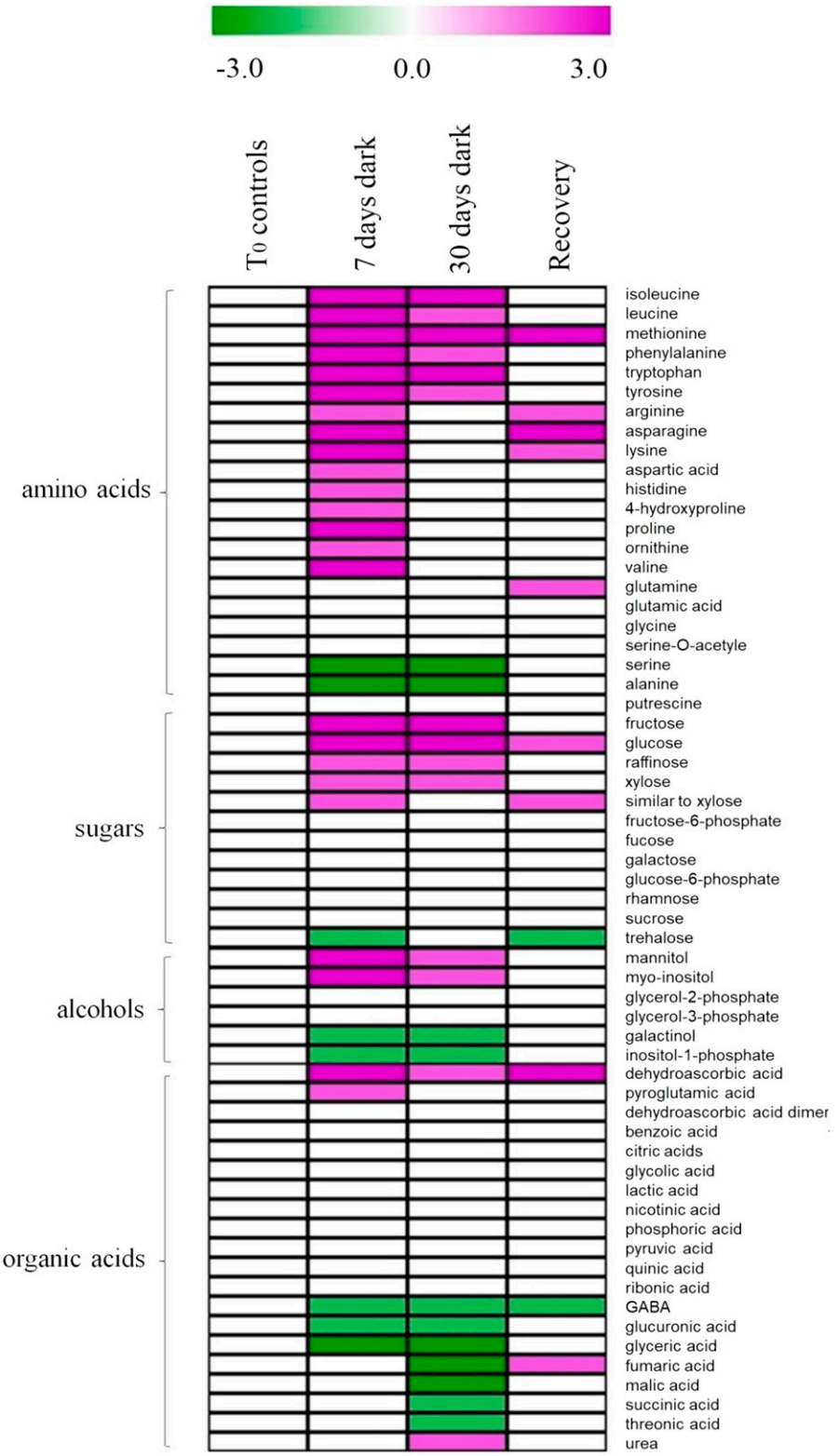

Figure 8. Changes in metabolite abundances of *H. rhodopensis* leaves during darkness and subsequent recovery. Green and magenta depict decreases and increases, respectively, in contents of metabolites (fold change, compared with the control plants grown under the photoperiod and sampled at the same time points). The data are means of six biological replicates.

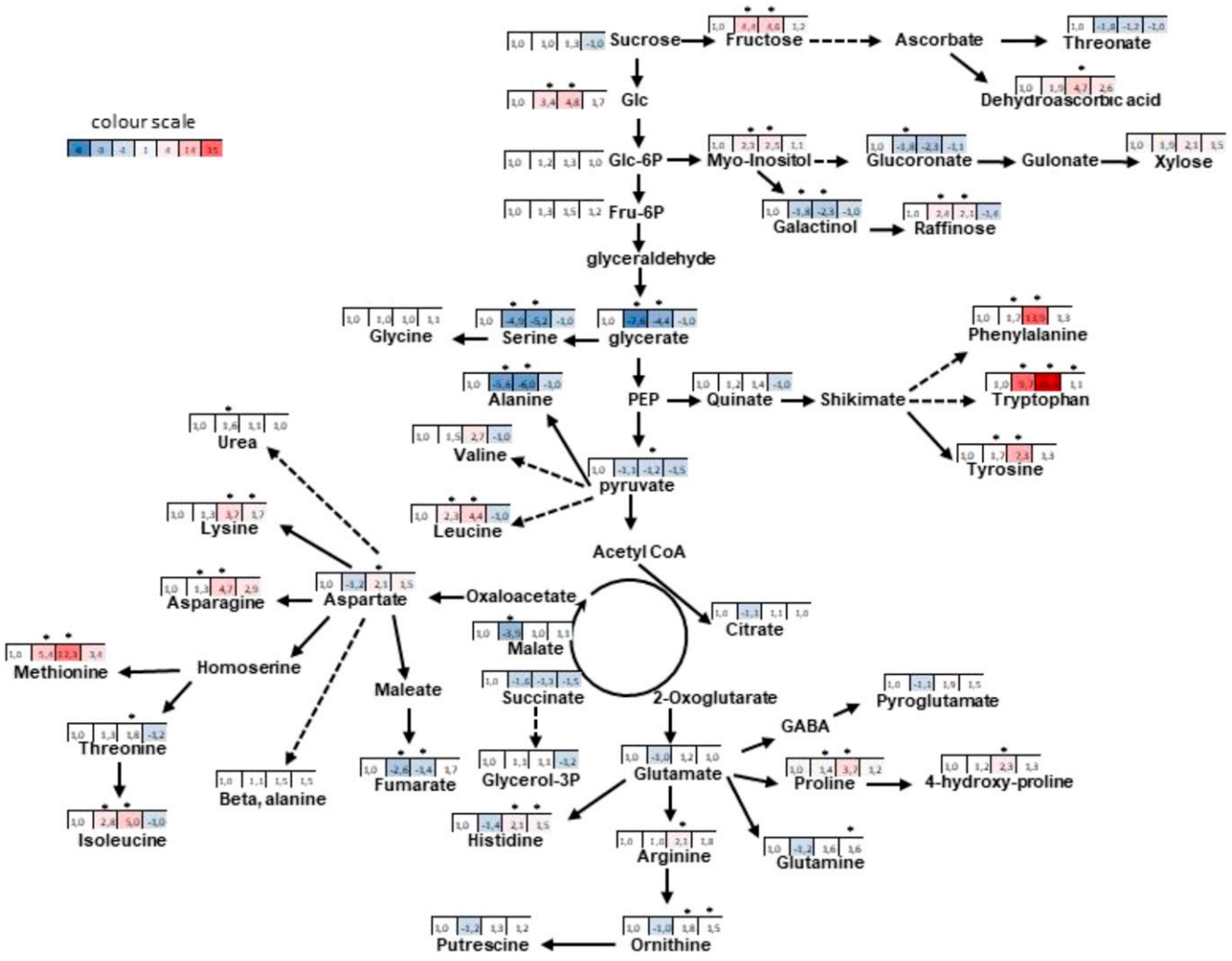

Figure 9. Major metabolic alterations of *H. rhodopensis* in response to long-term darkness and subsequent recovery. Blue and red depict decreases and increases in the content of metabolites, respectively (fold change, compared with the respective photoperiod controls). The data in the boxes are presented from left to right as follows: unstressed plants, 7 d of darkness, 30 d of darkness, and recovered plants. Statistical analysis was performed using Student's *t* test ($P < 0.05$). The data are means of six biological replicates. GABA, γ-Aminobutyric acid; PEP, phospho*enol*pyruvate.

including digalactosyldiacylglycerol (DGDG), monogalactosyldiacylglycerol (MGDG), phosphatidylcholine (PC), phosphatidylethanolamine, phosphatidylglycerol (PG), and sulfoquinovosyldiacylglycerol (SQDG) classes, were determined.

To achieve a comprehensive overview of the lipid modifications upon long-term darkness, we performed principal component analysis on the 143 annotated lipids. Principal components 1 and 2 accounted for 56% and 18% of the total variances between the samples. Overall, the principal component analysis showed clear separation between plants exposed to darkness and control plants grown under standard conditions. Plants from the recovery time point were in a distinct group (Supplemental Fig. S7).

More detailed analyses revealed that extended darkness induced notable changes in the lipidome, although some of the annotated lipids were invariant across the experiment (Fig. 10). For instance, around 25% of the annotated lipids, mostly belonging to the TAG class of neutral lipids, accumulated upon darkness but their abundances decreased upon recovery (7 d of light) (Supplemental Table S6). However, several other lipids, such as TAG 52:7, PC 34:5, and PC 34:4, were highly abundant following exposure to extended darkness and recovery. By contrast, the levels of several chloroplast lipids from the galactolipids MGDG and DGDG that constitute the bulk of membrane lipids in chloroplasts (about 30% of the annotated lipids), as well as PG and SQDG that are important to form the lipid bilayer of the thylakoid membrane classes, were reduced in darkness (especially during the 30-d dark period) but increased following recovery. For example, two polar lipids, PG 34:4 and PG 32:1, diminished in the dark condition but accumulated following the 1-week recovery.

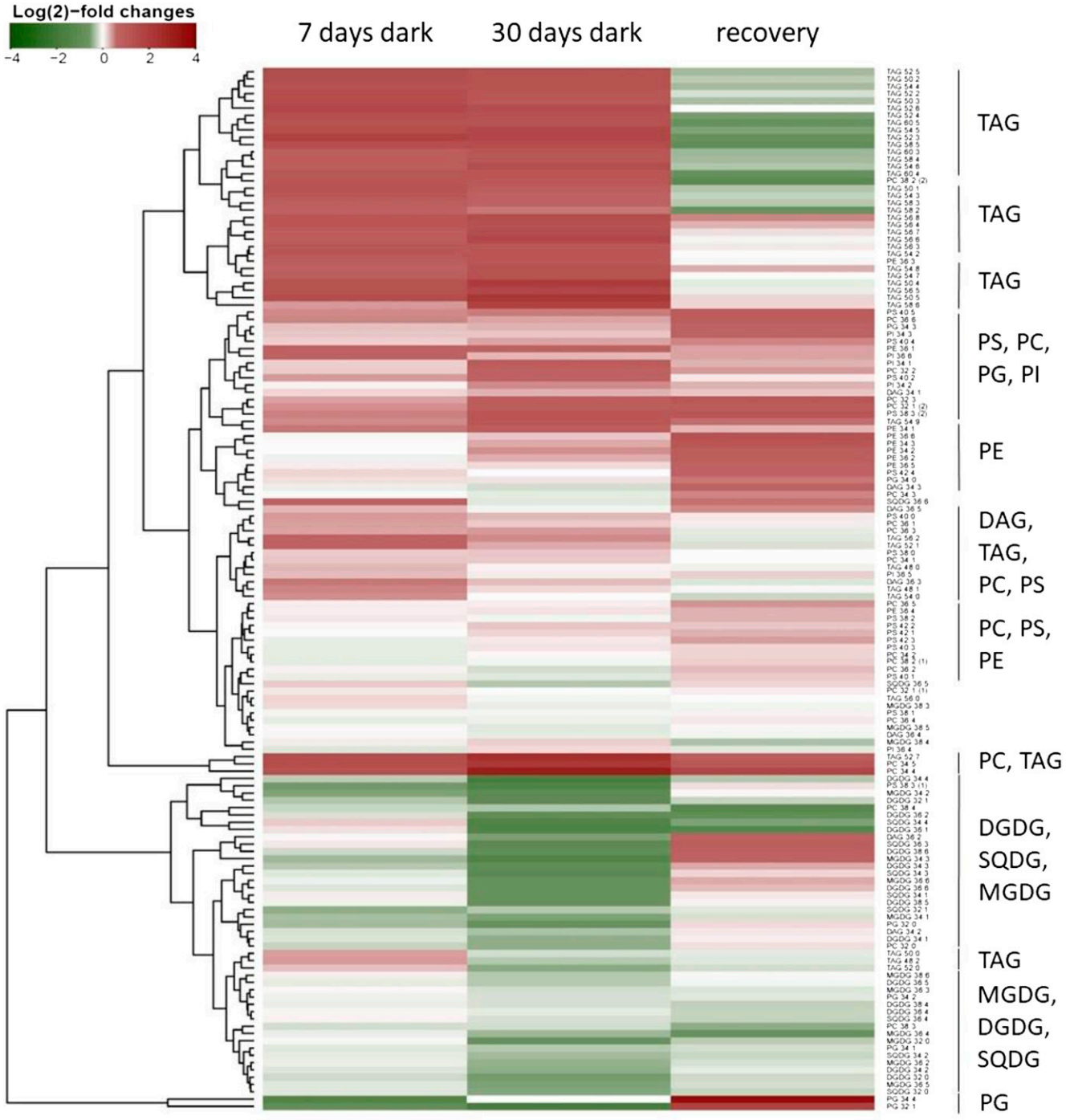

Figure 10. Changes in lipid abundances of *H. rhodopensis* leaves during darkness and subsequent recovery. Green and red depict decreases and increases, respectively, in lipid content. Values plotted are $\log_2$ fold change, where T0 values = 0. DAG, Diacylglycerol; PE, phosphatidylethanolamine; PI, phosphatidylinositol; PS, phosphatidylserine. The data are means of six biological replicates.

DISCUSSION

H. rhodopensis Can Tolerate Long Periods of Darkness

H. rhodopensis can withstand 30 d of complete darkness with just a small loss of chlorophyll and without any symptoms of cell death. This is a rare phenomenon among angiosperms, as long-term darkness induces energy starvation, premature senescence, and eventually cell death in many other angiosperm species (Ishizaki et al., 2005; Denev et al., 2012; Sakuraba et al., 2014; Song et al., 2014; Huo et al., 2015; Talla et al., 2016; Schwarz et al., 2017). It might be that some

angiosperm perennials, such as *H. rhodopensis*, are generally better adapted to low-intensity radiation than annual species and, therefore, might better tolerate long-term darkness, but more research is needed to support this hypothesis. We confirmed the sensitivity of Arabidopsis to prolonged darkness: under the experimental conditions used, Arabidopsis plants lost chlorophyll after 3 weeks of darkness and died, while *H. rhodopensis* plants retained most of its chlorophyll and remained viable even after 30 d of darkness.

Angiosperm species have the light-dependent protochlorophylide reductase (LPOR), a key enzyme in chlorophyll synthesis, while gymnosperms have both light-dependent and light-independent (DPOR) enzymes and can synthesize chlorophyll in darkness (Fujita and Bauer, 2000). In *H. rhodopensis*, one LPOR-encoding gene is repressed 4-fold and another is induced 2-fold in darkness. In other angiosperms, such as Arabidopsis and the gymnosperms Norway spruce (*Picea abies*) and Chinese fir (*Cunninghamia lanceolata*), *LPOR* is down-regulated in darkness (Stolárik et al., 2017; Xue et al., 2017). *DPOR* is less regulated in darkness: in *C. lanceolata*, one gene encoding a DPOR subunit is induced slightly, while the genes encoding the other two subunits are repressed slightly; in *P. abies*, all three genes are induced (Stolárik et al., 2017; Xue et al., 2017). However, the chlorophyll content in both gymnosperm species decreased to a greater extent than in *H. rhodopensis* (Stolárik et al., 2017; Xue et al., 2017).

Dark-induced chlorophyll degradation, senescence, and cell death are regulated by a number of TFs, other proteins, and microRNAs in Arabidopsis, while the genes and proteins controlling senescence and tolerance to darkness in *H. rhodopensis* are unknown (Ishizaki et al., 2005; Denev et al., 2012; Sakuraba et al., 2014; Song et al., 2014; Huo et al., 2015).

Despite the harsh conditions and lack of photosynthesis, the development of *H. rhodopensis* was not halted completely under complete darkness in our experiment. Plants continued to gain fresh weight in darkness, most likely due to the presence of Suc in the medium. Cell cycle genes were expressed in darkness at levels comparable to the expression levels of the control plants grown in light. Genes related to growth and development also were not repressed in darkness. A few genes encoding extensins, expansins, and xyloglucan endotransglycosylases, which are involved in cell wall extensibility and cell enlargement (Nieuwland et al., 2005; Sampedro and Cosgrove, 2005; Chebli and Geitmann, 2017), were even induced in darkness.

Interestingly, many chlorophyll catabolism genes were repressed in darkness in *H. rhodopensis*, especially those constituting the early steps of chlorophyll breakdown (*SGRL*, *NYC1*, and *PPH*), and the expression of two key genes involved in the porphyrin ring opening of pheophorbide *a* (*PAO* and *RCCR*) was not altered (Table II). This is in sharp contrast to dark-senescing species, where chlorophyll catabolism genes are induced (Kuai et al., 2018) and chlorophyll degradation occurs as a visible symptom of premature aging, followed by cell damage and eventually cell death (Pruzinská et al., 2005; Song et al., 2014). In Arabidopsis, where chlorophyll catabolism genes are induced and chlorophyll is degraded in darkness, the jasmonate-regulated TF MYC2 activates three chlorophyll catabolism/degradation genes, *PAO*, *NYC1*, and *SGR1*, by binding directly to their promoters (Zhu et al., 2015). In *H. rhodopensis*, neither the jasmonate pathway nor the MYC2 homolog is activated. In Arabidopsis and other dark-sensitive species, chlorophyll breakdown products (phyllobilins) accumulate and can be detected to follow the progression of senescence (Pruzinská et al., 2005; Christ et al., 2016). In *H. rhodopensis*, we were unable to identify the known chlorophyll catabolite products, with the exception of NCC_806, which also was present in control samples. This, together with the preserved chlorophyll content in darkness, collectively indicates that senescence is not triggered after 30 d of dark stress.

Transcriptional Reprogramming and Metabolome Reconfiguration during Darkness and Subsequent Recovery

As would be anticipated, the lack of light caused profound changes in gene expression (Supplemental Table S7). Most of the genes encoding TFs were unaltered in their expression, with only a small number of genes of this class being highly regulated in extended darkness (induced or repressed). The small number of altered TF genes makes them likely players in the massive transcriptional reprogramming observed in darkness.

One of the two most up-regulated genes exhibits sequence homology to a gene from Arabidopsis with similarity to a TF (TF domains) but an uncharacterized function, while most of the other *H. rhodopensis* TF genes are similar to genes that have been characterized previously. Two of the most up-regulated TF genes have similarities to Arabidopsis *ANAC029* and *WRKY33*, which are linked to senescence and autophagy, respectively (Lai et al., 2011; Trivellini et al., 2012). In Arabidopsis, darkness induces *ANAC029*, and mutation of this gene delays chlorophyll loss and senescence symptoms (Trivellini et al., 2012).

The induction of ethylene-responsive TFs indicates a possible role of the ethylene pathway in the adaptation to darkness. This could be 2-fold: ethylene signaling is important for growth in darkness (skotomorphogenesis) and for the activation of defense mechanisms against various abiotic stresses (Van de Poel et al., 2015). *H. rhodopensis* appears slightly etiolated in darkness, which could potentially be explained by the activation of ethylene signaling, although the activation of parallel stress pathways cannot be excluded.

Upon sensing darkness, *H. rhodopensis* responds by inducing the photoreceptor genes encoding phytochromes and cryptochromes as well as by down-regulating the phytochrome-interacting TF gene *PIF4*. The repression of *PIF* genes in *H. rhodopensis* by darkness is in contrast

Table II. Expression of chlorophyll catabolism genes

T0 are the unstressed controls at the beginning of the experiment. Values are Trimmed Mean of M (TMM) values, averages of three biological replicates. *SGR, STAY GREEN*; *SGRL, STAY GREEN-LIKE*; *NYC1, NON-YELLOW COLORING1*; *CHL, CHLOROPHYLLASE*; *PPH, PHEOPHYTINASE*; *PAO, PHEOPHORBIDE A OXYGENASE*; *RCCR, RED CHLOROPHYLL CATABOLITE REDUCTASE*; *HCAR, 7-HYDROXYMETHYL CHLOROPHYLL A REDUCTASE*.

Gene Identifier	Gene Name	TMM Values						
		T0 Controls	7 d of Light	30 d of Light	37 d of Light	7 d of Dark	30 d of Dark	7 d of Recovery
TRINITY_DN89389_c2_g1	SGR	3.10	3.94	3.90	5.22	8.53	9.80	6.01
TRINITY_DN101222_c0_g2	SGRL	15.52	13.25	13.25	13.10	7.11	8.34	16.86
TRINITY_DN110271_c6_g6	NYC1	25.42	23.50	21.08	24.22	6.95	6.80	30.42
TRINITY_DN73103_c0_g1	CHL	21.98	21.67	18.07	19.11	6.18	3.86	21.25
TRINITY_DN100094_c0_g1	PPH	20.60	20.45	17.14	16.76	6.27	3.79	25.84
TRINITY_DN89891_c1_g2	PAO	23.78	26.46	22.87	27.49	35.35	17.93	29.82
TRINITY_DN99068_c3_g1	RCCR	18.25	19.77	18.68	18.91	21.81	14.25	23.17
TRINITY_DN89814_c0_g1	HCAR	16.63	18.36	19.65	21.13	13.08	8.57	20.55

with the induction of these genes by darkness in Arabidopsis (Trivellini et al., 2012; Martín et al., 2016). Phytochromes are negative regulators of PIF proteins. PIFs, in turn, are transcriptional repressors of photomorphogenesis, and in Arabidopsis, both PIF4 and PIF5 are required for dark-induced senescence (Trivellini et al., 2012; Sakuraba et al., 2014). PIF4 and PIF5 activate the expression of the NAC TF *ORESARA1*, which is a positive regulator of dark-induced senescence (Sakuraba et al., 2014). Mutations in *PIF4*, as well as in *PIF3* and *PIF5*, delay the dark-induced senescence (Trivellini et al., 2012; Song et al., 2014). Hence, the up-regulation of phytochrome genes and the related repression of *PIFs* in darkness may serve to mitigate the detrimental effects of darkness and prevent dark-induced senescence in *H. rhodopensis*.

Although *H. rhodopensis* does not suffer from severe stress in darkness, the induction of several stress-related TF genes implies growth conditions that are far from optimal. The induction of two *H. rhodopensis* genes with similarities to heat shock factor genes resembles a response to heat and other abiotic stresses (Ohama et al., 2017), while the induction of a gene with similarity to *TGA1* resembles pathogen attack. Furthermore, the strong up-regulation of an *H. rhodopensis* gene with similarities to Arabidopsis *RD26* (*ANAC072*) resembles drought stress and senescence responses. In Arabidopsis, RD26 is induced by abiotic stresses, such as drought or darkness, and positively regulates senescence by stimulating chlorophyll degradation through the up-regulation of *SGR1*, an Mg chelatase that is a key regulatory gene in the early steps of chlorophyll degradation (Fujita et al., 2004; Li et al., 2016; Shimoda et al., 2016). *RD26* overexpressors exhibit accelerated age- and dark-induced senescence, while mutant plants have delayed senescence (Li et al., 2016). Additionally, RD26 inhibits brassinosteroid-regulated gene expression by antagonizing BRI1-ETHYL METHANESULFONATE-SUPPRESSOR1-mediated transcription, thus repressing brassinosteroid signaling and growth (Ye et al., 2017).

Several flowering-related TF genes, such as *COL2* and *COL4*, which are homologous to the flowering-time gene *CONSTANS*, were repressed in *H. rhodopensis*, which suggests an inhibition of flower development. Furthermore, the floral gene *RL1* was the most repressed among all down-regulated genes. Collectively, the down-regulation of the *H. rhodopensis* TF genes *GLK1*, *RD26*, *COL2*, and *COL4* may serve to inhibit developmental processes such as photomorphogenesis and flowering.

Down-Regulation of Photosynthesis and Photorespiration

Almost all photosynthesis-related genes were down-regulated in darkness, including genes encoding proteins from PSI and PSII, the light-harvesting complex, the Calvin cycle, and other photosynthesis-related proteins. The synthesis of all these proteins requires energy and carbon investment; thus, by minimizing their synthesis, *H. rhodopensis* may economize on valuable energy and nutrient resources. The down-regulation of photosynthesis by repression of photosynthesis-related genes but maintenance of most of the chlorophyll enables quick recovery upon reexposure to light.

The repression of *Rubisco* and other photosynthesis-related genes saves carbon and energy from the decreased levels of their respective proteins. The protein subunits of Rubisco and LIGHT-HARVESTING COMPLEX OF PHOTOSYSTEM II are the most abundant soluble and membrane proteins in plants (Ellis, 1979; Erb and Zarzycki, 2018); thus, any potential decrease in their quantity would have an impact on the energy and carbon balance. Furthermore, the repression of Rubisco decreases photorespiration, as less phosphoglycolate is produced. Key photorespiratory genes, such as phosphoglycolate phosphatase, catalase, and glycerate kinase, are repressed in prolonged darkness. This again saves energy and minimizes hydrogen peroxide production in peroxisomes. Further confirmation of the repression of the photorespiratory pathways in darkness comes from the decreased levels of Ser, the key intermediate of the pathway. Thus, both photosynthesis- and photorespiration-related genes are repressed in darkness, as they are no longer

required, and their shutdown saves valuable resources. The down-regulation of a number of chloroplast-related TFs and regulators, as well as degradation of the galctolipids SQDG and PG, also are in line with the overall shutdown of the chloroplast machinery.

Sugar and Lipid Metabolism in Darkness

Starch is the principal storage carbohydrate in most plants, being synthesized in plastids as a major product of photosynthesis. Prolonged darkness will ultimately lead to the exhaustion of starch and lipid reserves and may cause starvation. The repression of both starch-synthesizing (phosphoglucomutases, ADP-Glc pyrophosphorylases, and starch synthases) and starch-degrading (e.g. α- and β-amylases) genes supports the notion of starch depletion following long periods of darkness. The metabolome data revealed that Suc levels were unaltered during the dark treatment, while the monosaccharides Fru and Glc increased (Fig. 10). This is consistent with the up-regulation of Suc synthase genes. These responses seem to be specific to dark stress and are in contrast with the molecular responses of *H. rhodopensis* to desiccation, wherein a high accumulation of Suc occurs in parallel with the depletion of monosaccharides such as Glc and Fru (Gechev et al., 2013). Interestingly, Glc treatment can suppress the up-regulation of *PIF4* and *PIF5* in detached Arabidopsis inflorescences in darkness, thus mimicking *pif* mutations and delaying yellowing in darkness (Trivellini et al., 2012).

Lipids also are an important source of carbon and energy storage in plants, and lipid bodies accumulate upon inhibition of photosynthesis or extended darkness (Schwarz et al., 2017). The galactolipids MGDG and DGDG constitute the bulk of membrane lipids in chloroplasts and are essential as major structural components of the thylakoid membrane (Kobayashi and Wada, 2016). Moreover, neutral lipids have key functions in intracellular homeostasis and energy balance, especially under adverse conditions (Kunz et al., 2009; Gasulla et al., 2013; Fan et al., 2014). Under carbon starvation, fatty acids released from storage lipids, such as TAG, and/or membrane lipids are used as alternative substrates for respiration (Kunz et al., 2009). Long-term darkness resulting in the depletion of starch triggers the mobilization of lipid reserves, which is reflected by the induction of lipase genes. In our study, many lipid species, including MGDG, DGDG, PG, and SQDG, decrease notably in darkness, especially after 30 d, which suggests their usage as alternative carbon and energy sources. These four lipid classes constitute the bulk of the lipid bilayer of the chloroplast thylakoid membrane (Kobayashi and Wada, 2016), and even a small percentage of their total amount can provide enough energy and carbon to compensate for the shortages in darkness. In addition to the membrane lipids, other lipids (e.g. those of the wax layer) also may serve as alternative energy and carbon sources. In our experiment, one of the down-regulated lipid-related genes encodes an esterase/lipase similar to *AT5G33370*, which is involved in cuticle formation in Arabidopsis. A recent study on Arabidopsis plants exposed to darkness shows that fatty acids, such as MGDG and DGDG, released from thylakoid membranes are first incorporated into TAG, and the acyl groups derived from TAG hydrolysis are then degraded by β-oxidation in the peroxisomes (Fan et al., 2017). We noticed a substantial increase in many TAG species. Collectively, our data suggest the degradation of membrane lipids and their transformation into TAG as an alternative energy source. Another role for TAG during long-term darkness could be in limiting the generation of reactive oxygen species (ROS), especially toxic lipid hydroperoxides, which are observed in dark-senescing species (Kuramoto et al., 2012; Watanabe et al., 2013; Bailey et al., 2015; Fan et al., 2017). Disruption of the cytosolic lipase *SUGAR DEPENDENT1* in Arabidopsis, responsible for hydrolyzing TAGs, increases TAG accumulation and decreases the levels of hydrogen peroxide and malondialdehyde (indicators of oxidative stress and membrane damage, respectively) during long-term darkness (Fan et al., 2017). The accumulation of TAGs also was observed in *atg* mutant lines (Avin-Wittenberg et al., 2015). Recently, TAG accumulation was found to increase heat resistance (Mueller et al., 2017). Furthermore, the fatty acids released after the dark stress can serve in the buildup of other lipids during recovery.

Antioxidant Metabolism and ROS Homeostasis

The accumulation of ROS occurs as a consequence of many abiotic and biotic stresses and also is an important factor during senescence (Gadjev et al., 2006; Gechev et al., 2006). The up-regulation of many stress-related TFs and the increased dehydroascorbate levels in darkness collectively indicate that long-term darkness is a physiological stress condition. However, established gene markers for elevated hydrogen peroxide levels and oxidative stress, such as glutathione peroxidases and glutathione-*S*-transferases (Kovtun et al., 2000; Gechev et al., 2005), were not induced in *H. rhodopensis*. By contrast, most of these ROS marker genes as well as other antioxidant genes were either unaffected or repressed in darkness, and only a few antioxidant genes were induced.

One of the few induced genes encoded a glutathione reductase. Functional glutathione reductase is required for managing dark stress, as plants with decreased expression of *GLUTATHIONE REDUCTASE2* displayed a lower GSH/GSSG ratio and an early onset of age- and dark-induced senescence (Ding et al., 2016). Thus, the induction of glutathione reductase may contribute to adaptation to dark stress in *H. rhodopensis*.

Another up-regulated antioxidant gene encodes mitochondrial MnSOD. By contrast, the chloroplastic Cu/ZnSOD and FeSOD and a peroxisomal catalase were repressed. Under light, the chloroplasts and the peroxisomes are the main sites of ROS production,

while mitochondria play a minor yet important role (Gechev et al., 2006; Foyer and Noctor, 2013). The lack of photosynthesis and photorespiration in dark-treated *H. rhodopensis* is likely to considerably reduce the generation of ROS in chloroplasts and peroxisomes, eliminating the need for the strong expression of antioxidant-related genes and leaving the mitochondria as the main ROS generators in the cell. The increased ROS production in the mitochondria may be related to increased mitochondrial activity, which is needed to compensate for the lack of energy production in the chloroplasts. In addition, more ROS may be produced by acyl-CoA oxidase due to increased β-oxidation of fatty acids (Fan et al., 2017).

Mobilization of Alternative Energy and Nutrient Sources by Activation of the SnRK1 Pathway, Induction of Protein Degradation, and Autophagy

In our experiment, a number of *SUCROSE NON-FERMENTING1-RELATED PROTEIN KINASES* (*SnRK*) genes were notably up-regulated in darkness, suggesting that this signaling pathway is activated. Its activation, in turn, explains the activation of processes such as protein degradation and autophagy, both of which are essential for surviving long-term darkness.

SnRKs play key roles in plant responses to energy and nutrient starvation imposed by biotic and abiotic stresses (Baena-González et al., 2007; Kim et al., 2017). The SnRK1 pathway controls transcription reprogramming in response to darkness, sugar, and stress conditions (Baena-González et al., 2007). The SnRK1 pathway can activate protein, lipid, and cell wall degradation, induce autophagy, and at the same time repress processes such as protein, amino acid, and cell wall synthesis (Baena-González and Sheen, 2008). Overexpression of the SnRK1 catalytic subunit KIN10 enhances starvation tolerance, while *kin10 kin11* double mutants cannot reprogram their transcriptome in response to extended darkness (Baena-González et al., 2007).

The increased abundance of many amino acids (such as Ile, Leu, Met, Phe, Pro, and Trp) collectively suggests increased protein degradation. The free amino acids can be used as an alternative energy source as well as building blocks for the de novo synthesis of dark-inducible proteins. In Arabidopsis, amino acids can be used as alternative substrates for respiration under dark-imposed energy deprivation (Araújo et al., 2010; Engqvist et al., 2011). Further support for this notion comes from the observation that mutants with compromised degradation of branched-chain amino acids, such as Leu, Ile, and Val, exhibit early senescence upon prolonged dark treatment (Peng et al., 2015). Moreover, a significant increase in branched-chain and aromatic amino acids was reported in a recent study on the Arabidopsis leaf metabolome during darkness (Law et al., 2018).

A number of autophagy-related genes were significantly up-regulated following extended darkness, clearly indicating that autophagy was activated and suggesting a role of this process in mitigating the energy and nutrient shortage during long-term dark stress. In addition to genes encoding autophagy-related proteins (such as proteins with similarities to ATG13b and ATG18d), a gene encoding a TF with similarities to Arabidopsis WRKY33 was up-regulated in *H. rhodopensis* following the imposition of long-term darkness. WRKY33 has been shown to interact with the important autophagy protein ATG18a in Arabidopsis, and the *wrky33* mutant is compromised in autophagy and highly susceptible to necrotrophic fungal pathogens such as *Botrytis cinerea* and *Alternaria brassicicola* (Lai et al., 2011). In tomato (*Solanum lycopersicum*), the WRKY33 homolog regulates the expression of *ATG* genes during heat stress, and its silencing reduces the expression of *ATG* genes, autophagosome accumulation, and tolerance to heat stress (Zhou et al., 2014). Autophagy plays a role in dark-induced senescence, where it is important for lipid and protein degradation during darkness and their use as alternative nutrient and energy resources (Li et al., 2014). In *Micrasterias denticulata*, lipid bodies containing both neutral and polar lipids are degraded via autophagy during long-term darkness (Schwarz et al., 2017). More recently, Arabidopsis *atg* mutants compromised in autophagy showed impaired protein degradation and early senescence under extended darkness (Barros et al., 2017).

CONCLUSION

The desiccation-tolerant plant *H. rhodopensis* exhibits the ability to survive long-term darkness without switching on a senescence program or suffering any apparent damage. The typical degradation of chlorophyll induced by darkness in other species was minimal in *H. rhodopensis*, and the accumulation of chlorophyll degradation products was minor. In contrast to species that undergo dark-induced senescence, in which chlorophyll catabolism genes are induced, most of these genes were repressed or unaltered in *H. rhodopensis*. The adaptation to darkness involved specific transcriptional reprogramming and metabolic reconfigurations, which led to the repression of photosynthesis, photorespiration, and flowering but the activation of the SnRK1 and autophagy pathways. We propose that, in *H. rhodopensis*, proteins and polar lipids, such as MGDG, DGDG, PG, and SQDG, are degraded and eventually used as alternative sources of nitrogen, carbon, and energy.

MATERIALS AND METHODS

Plant Material and Stress Treatments

Haberlea rhodopensis plants were routinely propagated in vitro on McCown Woody medium (Duchefa Biochemie; pH 5.7) containing 2% (w/v) Suc and grown in a controlled-environment growth chamber in optimal conditions

(16 h of light/8 h of dark) under 30 to 35 µmol m^{-2} s^{-1} light intensity at 22°C ± 1°C. Two weeks prior to dark treatment, plants were transferred to fresh medium. Half of the plants were kept under the above conditions and used as controls. For the dark treatment, whole plants (at nonbolting/nonflowering stage) were subjected to darkness for 7 or 30 d, followed by a recovery period of 7 d under normal light conditions. At the indicated time points, rosette leaves were collected in a dark room illuminated with nonactinic green light and immediately frozen in liquid nitrogen. To exclude any interference from the circadian clock, samples were always taken at noon. Well-hydrated plants had an RWC of 85%. Desiccation was conducted both with plants grown under photoperiod and in darkness by removing the medium for 5 d until plants reached the air-dried state at an RWC of 5%. Rehydration was achieved for 5 d by returning the plants to the well-hydrated medium until the plants reached their original RWC.

Arabidopsis (*Arabidopsis thaliana*) plants from the accession Landsberg *erecta* were germinated on 0.6% (w/v) agar-solidified Murashige and Skoog medium (Murashige and Skoog, 1962) supplemented with 2% (w/v) Suc in a controlled-environment growth chamber under 35 µmol m^{-2} s^{-1} light intensity, 16-h-light/8-h-dark photoperiod, at 22°C ± 1°C. Two-week-old plants were subjected to darkness for 3, 5, 10, and 21 d, and material was collected for chlorophyll measurements.

Electrolyte Leakage Measurements

Electrolyte leakage was assessed by measuring the increase in conductivity with an HI 873 conductivity meter (Hanna Instruments). *H. rhodopensis* leaves from the different time points and conditions were washed briefly with ultrapure water (conductivity of 1 µS). The leaves were then incubated in ultrapure water for 10 min. The conductivity of the resultant solution was measured and compared with the total conductivity obtained after boiling the leaves.

Chlorophyll and Phyllobilin Determination

Chlorophyll pigments were extracted overnight in 80% (v/v) ice-cold acetone from 50 mg of frozen and powdered plant material. After centrifugation (10 min, 15,000*g*, and 4°C), supernatants were analyzed spectrophotometrically and chlorophyll content was calculated as micrograms of chlorophyll per milligram fresh weight (Lichtenthaler, 1987).

Phyllobilins were extracted (in triplicate) from powdered leaf material and analyzed by an ultra-performance liquid chromatograph (with a C18 reverse-phase column) coupled with a quadrupole-time-of-flight mass spectrometer (Bruker) using a recently established protocol for chlorophyll degradation products (Christ et al., 2016). NCC_806 was identified by screening of the obtained mass spectrometry (MS) spectra against an MS library that contains respective MS and tandem MS spectra of 16 phyllobilins (http://www.botinst.uzh.ch/en/research/physiology/horten/ms-library.html), as described (Christ et al., 2016).

Isolation of RNA and RNA-seq

Total RNA for RNA-seq was extracted from three biological replicates for dark-treated, light-recovered, and control plants using the RNeasy Plant Mini Kit (Qiagen) according to the manufacturer's instructions. RNA was treated with Turbo DNase (Ambion) to remove DNA contamination. RNA integrity was checked on 1% (w/v) agarose gels, and quantity and purity were analyzed with a NanoDrop ND-2000 spectrophotometer (Thermo Fisher Scientific). mRNA was prepared for sequencing by the Beijing Genome Institute. Briefly, oligo(dT) magnetic beads were used to isolate mRNA from total RNA; mRNA was fragmented and used for cDNA synthesis. The cDNA was used for ligation of the sequencing adapters and PCR amplification. During the quality-control steps of sequencing, an Agilent 2100 Bioanalyzer (Agilent Technologies) and an ABI StepOnePlus Real-Time PCR system (Thermo Fisher Scientific) were used for quantification and quality check. Paired-end sequencing of all samples was performed using an Illumina HiSeq 4000 to generate ~990 Million. 100-bp read pairs. Raw data obtained were filtered through the standard Illumina pipeline to get clean data. The clean reads were assessed for various quality metrics (Supplemental Table S1) using an in-house script and FastQC (https://www.bioinformatics.babraham.ac.uk/projects/fastqc/). Further filtering was not required.

Bioinformatics

De novo transcriptome assembly was performed using Trinity (version 2.2.0) with read normalization (maximum read coverage, 50; Grabherr et al., 2011). Cdhit-est (–c 0.95; Fu et al., 2012) was used to reduce redundancies in the assembly. Reads from all samples were used to obtain a pooled transcriptome. Different *k*-mer lengths were optimized to obtain best assembly at *k*-mer 31 (Supplemental Table S1). BUSCO assessment (Simão et al., 2015) for completeness of assembly was done using the embryophyta_odb9 data set (downloaded from http://busco.ezlab.org). The reads were pseudoaligned against the obtained assembly using kallisto (bootstraps, 100) to obtain abundance estimation (Bray et al., 2016). Counts were normalized to obtain TMM (Robinson and Oshlack, 2010). Transcripts with TMM > 1 in at least one sample were retained to filter out potential assembly artifacts. Gene-level expression was obtained from transcript-level counts based on transcripts to genes mapping by Trinity, and we compared these with the genes from the *Boea hygrometrica* genome (a close relative of *H. rhodopensis* from the same family, Gesneriaceae). The numbers we report for *H. rhodopensis* are very close to the numbers reported previously for *B. hygrometrica*. Open reading frames and respective peptide sequences were predicted using TransDecoder (http://transdecoder.github.io).

Functional annotation was carried out using the Trinotate pipeline using the filtered transcriptome and predicted peptide sequences as reference. A BLAST search was conducted against UniProt (Swissprot + TrEMBL) and NCBI nr databases (E value ≤ 1e-20; -max_hsps: 1; -max_target_seqs: 1) using taxonomy filter for Viridiplantae (Altschul et al., 1990; UniProt Consortium, 2017). Protein domains were predicted using HMMER against the Pfam database (Bateman et al., 2004; Finn et al., 2011). GO annotations were obtained by merging the annotations from BLAST against UniProt, NCBI nr, and Pfam searches. TFs were identified using results from PlantTFDB (Jin et al., 2017) and GO term GO:0003700 (TF activity, sequence-specific DNA binding). BLAST annotations from different databases (UniProt and NCBI nr) for multiple transcripts were merged to assign the most appropriate description (Swissprot being preferred over TrEMBL and then NCBI nr). The genes that had no annotations in any of these databases were considered as TRGs.

For gene expression analysis, the EdgeR package in Bioconductor was used for all combinations (Robinson and Oshlack, 2010). A false discovery rate (FDR) cutoff of less than 0.001 and a $\log_2$ fold change greater than 1 were used to identify DEGs. Heat maps and clustering for selected groups of genes were made using the pheatmap R package (Kolde, 2015). GO enrichment was done using GOSeq (Young et al., 2010), with an FDR cutoff of less than 0.01. Differentially expressed TFs were curated manually to obtain the selected set.

Gas Chromatography-Mass Spectrometry Analysis of Primary Metabolites

For the analysis of primary metabolites, gas chromatography-mass spectrometry (GC-MS) was used as follows. Approximately 50 mg of plant material from different time points was collected and immediately frozen in liquid nitrogen prior to storage at −80°C. The samples were homogenized using a ball mill precooled with liquid nitrogen and extracted in 730 µL of 100% methanol. Then, 650 µL from the extraction liquid was taken and transferred into a new Eppendorf tube, flowed by adding 375 µL of $CHCl_3$ and 650 µL of water. After centrifugation, the resulting supernatant was dried under vacuum, and the residue was derivatized for 120 min at 37°C (in 40 µL of 20 mg mL^{-1} methoxyamine hydrochloride in pyridine) followed by a 30-min treatment at 37°C with 70 µL of MSTFA. The GC-MS system used was a gas chromatograph coupled to a time-of-flight mass spectrometer (Leco Pegasus HT TOF-MS). An auto sampler Gerstel Multi Purpose system injected the samples. Helium was used as the carrier gas at a constant flow rate of 2 mL s^{-1}, and gas chromatography was performed on a 30-m DB-35 column. The injection temperature was 230°C, and the transfer line and ion source were set to 250°C. The initial temperature of the oven (85°C) increased at a rate of 15°C min^{-1} up to a final temperature of 360°C. After a solvent delay of 180 s, mass spectra were recorded at 20 scans s^{-1} with a mass-to-charge ratio 70 to 600 scanning range. Chromatograms and mass spectra were evaluated by using Chroma TOF 4.5 (Leco) and TagFinder 4.2 software (Lisec et al., 2006). Six biological replicates were used for the analysis. Ribitol was used as an internal standard.

Lipid Profiling

Lipids were extracted from six biological replicates using the MTBE method described by Giavalisco et al. (2011). Vacuum-dried organic phases

were processed using ultra-performance liquid chromatography (on a C8 reverse-phase column) coupled with Fourier transform mass spectrometry (exactive mass spectrometer; Thermo Fisher Scientific) in positive and negative ionization modes. Processing of chromatograms, peak detection, and integration were performed using REFINER MSH 10 (GeneData). Processing of mass spectrometry data included the removal of the fragmentation information, isotopic peaks, and chemical noise. Selected features were annotated using an in-house lipid database. Raw lipid intensities were log normalized, and the heat map of $\log_2$ fold changes between the corresponding treatments and controls was drawn using the heatmap.2 function in the R package gplots (Warnes et al., 2016; gplots: various R programming tools for plotting data; https://CRAN.R-project.org/package=gplots). Six biological replicates were used for the analysis. PC 34:0 was used as an internal standard.

Accession Number

RNA-seq data from this article can be found in the NCBI Bioproject database (www.ncbi.nlm.nih.gov/bioproject) under accession number PRJNA397835.

Supplemental Data

The following supplemental materials are available.

Supplemental Figure S1. Arabidopsis undergoes dark-induced senescence.

Supplemental Figure S2. Identification of the chlorophyll catabolite NCC_806 in *H. rhodopensis*.

Supplemental Figure S3. Pseudoalignment using kallisto for different assemblies of *k*-mers.

Supplemental Figure S4. Sample correlation matrix using all DEGs ($\log_2$ fold change ≥ 1, FDR ≤ 0.001).

Supplemental Figure S5. Heat map of all genes clustered in 50 *k*-means clusters using pheatmap.

Supplemental Figure S6. Principal component analysis of metabolite levels of *H. rhodopensis* during light, darkness, and subsequent recovery phases.

Supplemental Figure S7. Principal component analysis of lipid levels of *H. rhodopensis* during light, darkness, and subsequent recovery phases.

Supplemental Table S1. Sample details including sequencing read quality control.

Supplemental Table S2. List of DEGs at each time point.

Supplemental Table S3. GO enrichment of all DEGs at each time point using GOSeq.

Supplemental Table S4. List of all genes with similarity to TFs along with respective expression levels.

Supplemental Table S5. Metabolite profiling from GC-MS evaluated using Chroma TOF and TagFinder.

Supplemental Table S6. Lipid profiling from ultra-performance liquid chromatography-Fourier transform-mass spectrometry.

Supplemental Table S7. List of induced and repressed genes in all treatments/conditions.

ACKNOWLEDGMENTS

We thank Dr. Christian Kappel (University of Potsdam) and New Zealand Genomics Limited for providing the infrastructure for bioinformatics analysis.

Received January 18, 2018; accepted May 9, 2018; published May 22, 2018.

LITERATURE CITED

Altschul SF, Gish W, Miller W, Myers EW, Lipman DJ (1990) Basic local alignment search tool. J Mol Biol **215**: 403–410

Araújo WL, Ishizaki K, Nunes-Nesi A, Larson TR, Tohge T, Krahnert I, Witt S, Obata T, Schauer N, Graham IA, (2010) Identification of the 2-hydroxyglutarate and isovaleryl-CoA dehydrogenases as alternative electron donors linking lysine catabolism to the electron transport chain of *Arabidopsis* mitochondria. Plant Cell **22**: 1549–1563

Araújo WL, Ishizaki K, Nunes-Nesi A, Tohge T, Larson TR, Krahnert I, Balbo I, Witt S, Dörmann P, Graham IA, (2011) Analysis of a range of catabolic mutants provides evidence that phytanoyl-coenzyme A does not act as a substrate of the electron-transfer flavoprotein/electron-transfer flavoprotein:ubiquinone oxidoreductase complex in Arabidopsis during dark-induced senescence. Plant Physiol **157**: 55–69

Avin-Wittenberg T, Bajdzienko K, Wittenberg G, Alseekh S, Tohge T, Bock R, Giavalisco P, Fernie AR (2015) Global analysis of the role of autophagy in cellular metabolism and energy homeostasis in *Arabidopsis* seedlings under carbon starvation. Plant Cell **27**: 306–322

Baena-González E, Sheen J (2008) Convergent energy and stress signaling. Trends Plant Sci **13**: 474–482

Baena-González E, Rolland F, Thevelein JM, Sheen J (2007) A central integrator of transcription networks in plant stress and energy signalling. Nature **448**: 938–942

Bailey AP, Koster G, Guillermier C, Hirst EM, MacRae JI, Lechene CP, Postle AD, Gould AP (2015) Antioxidant role for lipid droplets in a stem cell niche of Drosophila. Cell **163**: 340–353

Barros JAS, Cavalcanti JHF, Medeiros DB, Nunes-Nesi A, Avin-Wittenberg T, Fernie AR, Araújo WL (2017) Autophagy deficiency compromises alternative pathways of respiration following energy deprivation in *Arabidopsis thaliana*. Plant Physiol **175**: 62–76

Bateman A, Coin L, Durbin R, Finn RD, Hollich V, Griffiths-Jones S, Khanna A, Marshall M, Moxon S, Sonnhammer EL, (2004) The Pfam protein families database. Nucleic Acids Res **32**: D138–D141

Benina M, Obata T, Mehterov N, Ivanov I, Petrov V, Toneva V, Fernie AR, Gechev TS (2013) Comparative metabolic profiling of *Haberlea rhodopensis*, *Thellungiella halophyla*, and *Arabidopsis thaliana* exposed to low temperature. Front Plant Sci **4**: 499

Bray NL, Pimentel H, Melsted P, Pachter L (2016) Near-optimal probabilistic RNA-seq quantification. Nat Biotechnol **34**: 525–527

Chebli Y, Geitmann A (2017) Cellular growth in plants requires regulation of cell wall biochemistry. Curr Opin Cell Biol **44**: 28–35

Christ B, Hauenstein M, Hörtensteiner S (2016) A liquid chromatography-mass spectrometry platform for the analysis of phyllobilins, the major degradation products of chlorophyll in *Arabidopsis thaliana*. Plant J **88**: 505–518

Denev I, Stefanov D, Terashima I (2012) Preservation of integrity and activity of *Haberlea rhodopensis* photosynthetic apparatus during prolonged light deprivation. Physiol Plant **146**: 121–128

Ding S, Wang L, Yang Z, Lu Q, Wen X, Lu C (2016) Decreased glutathione reductase2 leads to early leaf senescence in Arabidopsis. J Integr Plant Biol **58**: 29–47

Ellis RJ (1979) The most abundant protein in the world. Trends Biochem Sci **4**: 241–244

Engqvist MK, Kuhn A, Wienstroer J, Weber K, Jansen EE, Jakobs C, Weber AP, Maurino VG (2011) Plant D-2-hydroxyglutarate dehydrogenase participates in the catabolism of lysine especially during senescence. J Biol Chem **286**: 11382–11390

Erb TJ, Zarzycki J (2018) A short history of RubisCO: the rise and fall (?) of nature's predominant CO2 fixing enzyme. Curr Opin Biotechnol **49**: 100–107

Fan J, Yan C, Roston R, Shanklin J, Xu C (2014) *Arabidopsis* lipins, PDAT1 acyltransferase, and SDP1 triacylglycerol lipase synergistically direct fatty acids toward β-oxidation, thereby maintaining membrane lipid homeostasis. Plant Cell **26**: 4119–4134

Fan J, Yu L, Xu C (2017) A central role for triacylglycerol in membrane lipid breakdown, fatty acid β-oxidation, and plant survival under extended darkness. Plant Physiol **174**: 1517–1530

Finn RD, Clements J, Eddy SR (2011) HMMER web server: interactive sequence similarity searching. Nucleic Acids Res**39**: W29–W37

Foyer CH, Noctor G (2013) Redox signaling in plants. Antioxid Redox Signal **18**: 2087–2090

Fu L, Niu B, Zhu Z, Wu S, Li W (2012) CD-HIT: accelerated for clustering the next-generation sequencing data. Bioinformatics **28**: 3150–3152 10.1093/bioinformatics/bts56523060610

Fujita Y, Bauer CE (2000) Reconstitution of light-independent protochlorophyllide reductase from purified bchl and BchN-BchB subunits: in vitro confirmation of nitrogenase-like features of a bacteriochlorophyll biosynthesis enzyme. J Biol Chem **275**: 23583–23588

Fujita M, Fujita Y, Maruyama K, Seki M, Hiratsu K, Ohme-Takagi M, Tran LS, Yamaguchi-Shinozaki K, Shinozaki K (2004) A dehydration-induced NAC protein, RD26, is involved in a novel ABA-dependent stress-signaling pathway. Plant J **39**: 863–876

Gadjev I, Vanderauwera S, Gechev TS, Laloi C, Minkov IN, Shulaev V, Apel K, Inzé D, Mittler R, Van Breusegem F (2006) Transcriptomic footprints disclose specificity of reactive oxygen species signaling in Arabidopsis. Plant Physiol **141**: 436–445

Gasulla F, Vom Dorp K, Dombrink I, Zähringer U, Gisch N, Dörmann P, Bartels D (2013) The role of lipid metabolism in the acquisition of desiccation tolerance in *Craterostigma plantagineum*: a comparative approach. Plant J **75**: 726–741

Gechev TS, Minkov IN, Hille J (2005) Hydrogen peroxide-induced cell death in Arabidopsis: transcriptional and mutant analysis reveals a role of an oxoglutarate-dependent dioxygenase gene in the cell death process. IUBMB Life **57**: 181–188

Gechev TS, Van Breusegem F, Stone JM, Denev I, Laloi C (2006) Reactive oxygen species as signals that modulate plant stress responses and programmed cell death. BioEssays **28**: 1091–1101

Gechev TS, Dinakar C, Benina M, Toneva V, Bartels D (2012) Molecular mechanisms of desiccation tolerance in resurrection plants. Cell Mol Life Sci **69**: 3175–3186

Gechev TS, Benina M, Obata T, Tohge T, Sujeeth N, Minkov I, Hille J, Temanni MR, Marriott AS, Bergström E, (2013) Molecular mechanisms of desiccation tolerance in the resurrection glacial relic *Haberlea rhodopensis*. Cell Mol Life Sci **70**: 689–709

Georgieva K, Rapparini F, Bertazza G, Mihailova G, Sárvári É, Solti Á, Keresztes Á (2017) Alterations in the sugar metabolism and in the vacuolar system of mesophyll cells contribute to the desiccation tolerance of *Haberlea rhodopensis* ecotypes. Protoplasma **254**: 193–201

Giarola V, Krey S, Frerichs A, Bartels D (2015) Taxonomically restricted genes of *Craterostigma plantagineum* are modulated in their expression during dehydration and rehydration. Planta **241**: 193–208

Giavalisco P, Li Y, Matthes A, Eckhardt A, Hubberten HM, Hesse H, Segu S, Hummel J, Köhl K, Willmitzer L (2011) Elemental formula annotation of polar and lipophilic metabolites using (13) C, (15) N and (34) S isotope labelling, in combination with high-resolution mass spectrometry. Plant J **68**: 364–376

Grabherr MG, Haas BJ, Yassour M, Levin JZ, Thompson DA, Amit I, Adiconis X, Fan L, Raychowdhury R, Zeng Q, (2011) Full-length transcriptome assembly from RNA-Seq data without a reference genome. Nat Biotechnol **29**: 644–652

Hörtensteiner S (2013) Update on the biochemistry of chlorophyll breakdown. Plant Mol Biol **82**: 505–517

Huo X, Wang C, Teng Y, Liu X (2015) Identification of miRNAs associated with dark-induced senescence in Arabidopsis. BMC Plant Biol **15**: 266

Ishizaki K, Larson TR, Schauer N, Fernie AR, Graham IA, Leaver CJ (2005) The critical role of *Arabidopsis* electron-transfer flavoprotein:ubiquinone oxidoreductase during dark-induced starvation. Plant Cell **17**: 2587–2600

Jin J, Tian F, Yang DC, Meng YQ, Kong L, Luo J, Gao G (2017) PlantTFDB 4.0: toward a central hub for transcription factors and regulatory interactions in plants. Nucleic Acids Res **45**: D1040–D1045

Kim GD, Cho YH, Yoo SD (2017) Regulatory functions of cellular energy sensor SNF1-Related Kinase1 for leaf senescence delay through *ETHYLENE-INSENSITIVE3* repression. Sci Rep **7**: 3193

Kobayashi K, Wada H (2016) Role of lipids in chloroplast biogenesis. Subcell Biochem **86**: 103–125

Kolde, R. (2015). pheatmap: Pretty Heatmaps. R package version 1.0. 8.

Kovtun Y, Chiu WL, Tena G, Sheen J (2000) Functional analysis of oxidative stress-activated mitogen-activated protein kinase cascade in plants. Proc Natl Acad Sci USA **97**: 2940–2945

Kuai B, Chen J, Hörtensteiner S (2018) The biochemistry and molecular biology of chlorophyll breakdown. J Exp Bot **69**: 751–767

Kunz HH, Scharnewski M, Feussner K, Feussner I, Flügge UI, Fulda M, Gierth M (2009) The ABC transporter PXA1 and peroxisomal beta-oxidation are vital for metabolism in mature leaves of *Arabidopsis* during extended darkness. Plant Cell **21**: 2733–2749

Kuramoto K, Okamura T, Yamaguchi T, Nakamura TY, Wakabayashi S, Morinaga H, Nomura M, Yanase T, Otsu K, Usuda N, (2012) Perilipin 5, a lipid droplet-binding protein, protects heart from oxidative burden by sequestering fatty acid from excessive oxidation. J Biol Chem **287**: 23852–23863

Lai Z, Wang F, Zheng Z, Fan B, Chen Z (2011) A critical role of autophagy in plant resistance to necrotrophic fungal pathogens. Plant J **66**: 953–968

Law SR, Chrobok D, Juvany M, Delhomme N, Lindén P, Brouwer B, Ahad A, Moritz T, Jansson S, Gardestrom P, (2018) Darkened leaves use different metabolic strategies for senescence and survival. Plant Physiol **177**: 132–15010.1104/pp.18.00062

Li F, Chung T, Vierstra RD (2014) AUTOPHAGY-RELATED11 plays a critical role in general autophagy- and senescence-induced mitophagy in *Arabidopsis*. Plant Cell **26**: 788–807

Li S, Gao J, Yao L, Ren G, Zhu X, Gao S, Qiu K, Zhou X, Kuai B (2016) The role of ANAC072 in the regulation of chlorophyll degradation during age- and dark-induced leaf senescence. Plant Cell Rep **35**: 1729–1741

Lichtenthaler HK (1987) Chlorophylls and carotenoids: pigments of photosynthetic biomembranes. Methods Enzymol **148**: 350–382

Lisec J, Schauer N, Kopka J, Willmitzer L, Fernie AR (2006) Gas chromatography mass spectrometry-based metabolite profiling in plants. Nat Protoc **1**: 387–396

Martín G, Leivar P, Ludevid D, Tepperman JM, Quail PH, Monte E (2016) Phytochrome and retrograde signalling pathways converge to antagonistically regulate a light-induced transcriptional network. Nat Commun **7**: 11431

Mueller SP, Unger M, Guender L, Fekete A, Mueller MJ (2017) Phospholipid:diacylglycerol acyltransferase-mediated triacylglyerol synthesis augments basal thermotolerance. Plant Physiol **175**: 486–497

Murashige T, Skoog F (1962) A revised medium for rapid growth and bioassays with tobacco tissue cultures. Physiol Plant **15**: 473–497

Nieuwland J, Feron R, Huisman BA, Fasolino A, Hilbers CW, Derksen J, Mariani C (2005) Lipid transfer proteins enhance cell wall extension in tobacco. Plant Cell **17**: 2009–2019

Ohama N, Sato H, Shinozaki K, Yamaguchi-Shinozaki K (2017) Transcriptional regulatory network of plant heat stress response. Trends Plant Sci **22**: 53–65

Peng C, Uygun S, Shiu SH, Last RL (2015) The impact of the branched-chain ketoacid dehydrogenase complex on amino acid homeostasis in Arabidopsis. Plant Physiol **169**: 1807–1820

Pruzinská A, Tanner G, Aubry S, Anders I, Moser S, Müller T, Ongania KH, Kräutler B, Youn JY, Liljegren SJ, (2005) Chlorophyll breakdown in senescent Arabidopsis leaves: characterization of chlorophyll catabolites and of chlorophyll catabolic enzymes involved in the degreening reaction. Plant Physiol **139**: 52–63

Robinson MD, Oshlack A (2010) A scaling normalization method for differential expression analysis of RNA-seq data. Genome Biol **11**: R25

Sakuraba Y, Jeong J, Kang MY, Kim J, Paek NC, Choi G (2014) Phytochrome-interacting transcription factors PIF4 and PIF5 induce leaf senescence in Arabidopsis. Nat Commun **5**: 4636

Sampedro J, Cosgrove DJ (2005) The expansin superfamily. Genome Biol **6**: 242

Schwarz V, Andosch A, Geretschläger A, Affenzeller M, Lütz-Meindl U (2017) Carbon starvation induces lipid degradation via autophagy in the model alga Micrasterias. J Plant Physiol **208**: 115–127

Shimoda Y, Ito H, Tanaka A (2016) Arabidopsis STAY-GREEN, Mendel's green cotyledon gene, encodes magnesium-dechelatase. Plant Cell **28**: 2147–216010.1105/tpc.16.00428

Simão FA, Waterhouse RM, Ioannidis P, Kriventseva EV, Zdobnov EM (2015) BUSCO: assessing genome assembly and annotation completeness with single-copy orthologs. Bioinformatics **31**: 3210–3212

Song Y, Yang C, Gao S, Zhang W, Li L, Kuai B (2014) Age-triggered and dark-induced leaf senescence require the bHLH transcription factors PIF3, 4, and 5. Mol Plant **7**: 1776–1787

Stolárik T, Hedtke B, Šantrůček J, Ilík P, Grimm B, Pavlovič A (2017) Transcriptional and post-translational control of chlorophyll biosynthesis by dark-operative protochlorophyllide oxidoreductase in Norway spruce. Photosynth Res **132**: 165–179; erratum **Stolárik T, Hedtke B, Šantrůček J, Ilík P, Grimm B, Pavlovič A** (2017) Photosynth Res **132**: 181

Talla SK, Panigrahy M, Kappara S, Nirosha P, Neelamraju S, Ramanan R (2016) Cytokinin delays dark-induced senescence in rice by maintaining the chlorophyll cycle and photosynthetic complexes. J Exp Bot **67**: 1839–1851

Trivellini A, Jibran R, Watson LM, O'Donoghue EM, Ferrante A, Sullivan KL, Dijkwel PP, Hunter DA (2012) Carbon deprivation-driven transcriptome

reprogramming in detached developmentally arresting Arabidopsis inflorescences. Plant Physiol **160**: 1357–1372

UniProt Consortium (2017) UniProt: the universal protein knowledgebase. Nucleic Acids Res **45**: D158–D169

Van de Poel B, Smet D, Van Der Straeten D (2015) Ethylene and hormonal cross talk in vegetative growth and development. Plant Physiol **169**: 61–72

Warnes GR, Bolker B, Bonebakker L, Gentleman R, Liaw WH, Lumley T, Maechler M, Magnusson A, Moeller S, Schwartz M, Venables B (2016) gplots: various R programming tools for plotting data. R package version 3.0. 1. The Comprehensive R Archive Network.

Watanabe M, Balazadeh S, Tohge T, Erban A, Giavalisco P, Kopka J, Mueller-Roeber B, Fernie AR, Hoefgen R (2013) Comprehensive dissection of spatiotemporal metabolic shifts in primary, secondary, and lipid metabolism during developmental senescence in Arabidopsis. Plant Physiol **162**: 1290–1310

Xiao L, Yang G, Zhang L, Yang X, Zhao S, Ji Z, Zhou Q, Hu M, Wang Y, Chen M, (2015) The resurrection genome of *Boea hygrometrica*: a blueprint for survival of dehydration. Proc Natl Acad Sci USA **112**: 5833–5837

Xue X, Wang Q, Qu Y, Wu H, Dong F, Cao H, Wang HL, Xiao J, Shen Y, Wan Y (2017) Development of the photosynthetic apparatus of Cunninghamia lanceolata in light and darkness. New Phytol **213**: 300–313

Ye H, Liu S, Tang B, Chen J, Xie Z, Nolan TM, Jiang H, Guo H, Lin HY, Li L, (2017) RD26 mediates crosstalk between drought and brassinosteroid signalling pathways. Nat Commun **8**: 14573

Young MD, Wakefield MJ, Smyth GK, Oshlack A (2010) Gene Ontology analysis for RNA-seq: accounting for selection bias. Genome Biol **11**: R14

Zhou J, Wang J, Yu JQ, Chen Z (2014) Role and regulation of autophagy in heat stress responses of tomato plants. Front Plant Sci **5**: 174

Zhu X, Chen J, Xie Z, Gao J, Ren G, Gao S, Zhou X, Kuai B (2015) Jasmonic acid promotes degreening via MYC2/3/4- and ANAC019/055/072-mediated regulation of major chlorophyll catabolic genes. Plant J **84**: 597–610